Journal of Mathematical Psychology 105 (2021) 102594

Contents lists available at ScienceDirect

Journal of Mathematical Psychology

journal homepage: www.elsevier.com/locate/jmp

Attention as a source of variability in decision-making: Accounting for overall-value effects with diffusion models

Blair R.K. Shevlin [a], Ian Krajbich [a,b,*]

[a] The Ohio State University, Department of Psychology, Columbus, OH 43210, USA
[b] The Ohio State University, Department of Economics, Columbus, OH 43210, USA

ARTICLE INFO

Article history:
Received 22 August 2020
Received in revised form 20 July 2021
Accepted 30 August 2021
Available online 6 October 2021

Keywords:
Attention
Drift diffusion
Overall value
Response time
Eye tracking
Decision making

ABSTRACT

Research has demonstrated that value-based decisions depend on not only the relative value difference between options, but also their overall value. In particular, response times tend to decrease as the overall (summed) value of the options increase. Standard sequential sampling models such as the diffusion model can account for this fact by assuming that decision thresholds or noise vary with overall value. Alternatively, gaze-based models that incorporate eye-tracking data can accommodate this overall-value effect directly as a consequence of the multiplicative relationship between gaze and option value. We compare the fit of non-gaze diffusion models to data simulated with a multiplicative-gaze model. The results show how parameters related to decision thresholds or noise will vary as a function of overall value, even when there is no such variability in the data generating process. In empirical data, we find similar patterns where decision thresholds, noise, or non-decision time seem to vary with overall value. Our results reveal that specific patterns in standard diffusion model parameters can arise from a latent process of gaze-dependent evidence accumulation.

1. Introduction

Does the overall attractiveness of the options in a choice-set influence the decision-making process? The predominant view is that this "overall value" (OV) should not affect the decision process; the importance of a decision should depend only on the subjective-value (i.e., utility) difference between the available options (Tversky & Kahneman, 1979; Von Neumann & Morgenstern, 1944; Webb, 2018). This is because the relative value difference is what the decision-maker stands to gain by selecting the best option, relative to the other options. The value difference between the options also determines the ease of making decisions because larger value differences make it easier to discriminate between the options and identify the best one. The value-based decision-making literature is replete with examples demonstrating decision-makers' proficiency at quickly discriminating between unlike options (Chabris, Morris, Taubinsky, Laibson, & Schuldt, 2009; Clithero, 2018; Dutilh & Rieskamp, 2016; Jamieson & Petrusic, 1977; Konovalov & Krajbich, 2019; Krajbich, Armel, & Rangel, 2010; Milosavljevic, Malmaud, Huth, Koch, & Rangel, 2010). The fact that response times (RT) are shorter for decisions involving options that are on opposite ends of the value scale seems almost lawlike in nature.

In contrast, some researchers have noted that OV also impacts the decision process. In particular, the sum of the options' values tends to correlate negatively with RT. In other words, high OV decisions tend to be faster than low OV decisions (Fontanesi, Gluth, Spektor, & Rieskamp, 2019; Hunt et al., 2012; Pirrone, Azab, Hayden, Stafford and Marshall, 2018; Pirrone, Wen and Li, 2018; Polanía, Krajbich, Grueschow, & Ruff, 2014; Smith & Krajbich, 2018). In a particularly evocative examination of this effect, Pirrone, Azab et al. (2018) studied rhesus monkeys choosing between colored squares, each representing a different quantity of juice. The researchers included occasional trials with two identical options. They found that RTs were shorter for choices between two identically large quantities of juice than for two identically small quantities of juice.

Interestingly, there are analogous effects in perceptual decision-making, where researchers have noted that decisions involving high-magnitude stimuli tend to be fast (Bose, Bottom, Reina, & Marshall, 2020; Polanía et al., 2014; Ratcliff, Voskuilen and Teodorescu, 2018; Teodorescu, Moran, & Usher, 2016). For both magnitude and OV effects, the total stimulus intensity (e.g., numbers of dots, summed value, etc.) decreases RT while inconsistently impacting accuracy. In the same article by Pirrone, Azab et al. (2018) discussed above, the authors also studied humans completing a brightness discrimination task in which participants were required to indicate which of two grayscale patches was brighter. Embedded in this task were trials where both alternatives were of equal luminance. The researchers found

* Corresponding author at: The Ohio State University, Department of Psychology, Columbus, OH 43210, USA.
E-mail address: krajbich.1@osu.edu (I. Krajbich).

https://doi.org/10.1016/j.jmp.2021.102594
0022-2496/

that participants responded faster when choosing between high-equal-luminance options than low-equal-luminance options.

The literature has struggled to understand these OV effects from the perspective of sequential sampling models (SSM). Sequential sampling models, in particular the drift diffusion (or diffusion decision) model (DDM; e.g., Ratcliff & McKoon, 2008), have become canonical models for the decision process in both value-based and perceptual domains. In the DDM, the decision-maker evaluates the options, generating and accumulating noisy evidence for each, until one option accumulates enough evidence to be chosen. A common assumption among researchers employing these models is that the rate of evidence accumulation (the *drift rate*) depends on differences between options, and not the values of each option independently (Krajbich et al., 2010; Milosavljevic et al., 2010; Ratcliff, Voskuilen, Teodorescu, 2018; Roe, Busemeyer, & Townsend, 2001). This assumption follows from the fact that the DDM generates a choice function that is mathematically identical to classic logit models of choice that are based only on utility differences (Webb, 2018). Thus, standard variants of the DDM do not have a specific mechanism to capture OV effects.

Nevertheless, researchers have explored methods for using DDM parameters to accommodate stimulus magnitude effects in perceptual decision-making. In one study on perceptual decision-making, Ratcliff, Voskuilen, Teodorescu (2018) found that allowing either across-trial variability in drift rate (or the standard deviation of diffusion noise) to increase linearly with stimulus magnitude enabled it to better account for magnitude effects. Additionally, there are several other SSMs that share the assumption that within-trial variability increases with stimulus magnitude (Bose et al., 2020; Brunton, Botvinick, & Brody, 2013; Hunt et al., 2012; Kvam & Pleskac, 2016; Smith & Ratcliff, 2009; Teodorescu et al., 2016).

Other studies have allowed boundary separation to vary based on stimulus features, such as OV. Boundary separation indexes the decision criterion, the quantity of evidence a decision-maker requires before selecting an alternative. Typically, boundary separation is thought to be fixed before the onset of a trial (Ratcliff & McKoon, 2008; although, this assumption has been challenged by empirical work on cognitive control, see Botvinick, Braver, Barch, Carter, & Cohen, 2001; Cavanagh et al., 2011; Shenhav, Botvinick, & Cohen, 2013; Vassena, Deraeve, & Alexander, 2020). Nonetheless, some researchers have allowed boundary separation to decrease with higher OV, which reduces RT with only small decrements in accuracy (Cavanagh, Wiecki, Kochar, & Frank, 2014; Fontanesi et al., 2019; Pirrone, Azab et al., 2018; Pirrone, Wen et al., 2018).

These studies relax the common assumption that boundary separation and the variability in drift rate are constant across trials (Ratcliff, 1978; Ratcliff & Tuerlinckx, 2002). While these models are able to account for choice and RT patterns in the data, they are deviations from how DDMs are typically used.

Here, we propose an alternative explanation for OV effects based on existing variants of the DDM that have proven useful in explaining other patterns in human behavior. We refer in particular to DDMs with drift rates that incorporate gaze amplification of value (or other stimulus features; Tavares, Perona, & Rangel, 2017). The attentional DDM (aDDM) is the first of these variants (Krajbich et al., 2010; Smith & Krajbich, 2018; Smith, Krajbich, & Webb, 2019), but there exist many others (Amasino, Sullivan, Kranton, & Huettel, 2019; Ashby, Jekel, Dickert, & Glöckner, 2016; Fisher, 2017; Glickman et al., 2019; Sepulveda et al., 2020; Thomas, Molter, Krajbich, Heekeren, & Mohr, 2019; Towal, Mormann, & Koch, 2013; Westbrook et al., 2020).

In these models, drift rates are a function of the difference in the options' subjective values, which are scaled by gaze-based weights. This multiplicative, gaze-based mechanism has two behavioral consequences. First, it predicts that more gaze to an option increases its probability of being chosen, particularly for high-value options (controlling for relative value differences). Second, it predicts that high OV decisions will be faster due to bigger shifts in the drift rate associated with shifts in gaze.

Many studies have confirmed the relationship between gaze allocation and choice (Krajbich, 2019; Fig. 1A–B). There are clear correlations between gaze and choice, as well as some evidence that exogenously manipulating visual attention can bias choice (Armel, Beaumel, & Rangel, 2008; Gwinn, Leber, & Krajbich, 2019; Pärnamets et al., 2015; Shimojo, Simion, Shimojo, & Scheier, 2003; Tavares et al., 2017; but see Ghaffari & Fiedler, 2018; Newell & Le Pelley, 2018). Smith et al. (2019) specifically tested the multiplicative-gaze hypothesis across six datasets, finding consistent support for a multiplicative relationship between gaze and subjective value (Fig. 1C). Therefore, the advantage of this particular account is that it explains two patterns in the data (RT and gaze-weighted effects on choice) rather than just one (RT).

While this past work has qualitatively established that gaze-weighted DDMs produce OV effects, it is still unclear whether they produce the particular patterns in behavior that would correspond to increased drift/diffusion variability or decreased boundary separation with increased OV. That is what we set out to test in this paper.

These tests are important because eye-tracking data is not always available, particularly in older research. Thus, we need to know specifically what kinds of patterns in standard DDM parameters could, in principle, be explained by an underlying gaze-dependent DDM. One could look for these patterns in existing DDM publications and revisit those paradigms with eye-tracking and gaze-dependent DDMs. This in turn could lead to new insights into the phenomena studied in those papers.

To examine how the standard DDM might account for gaze-dependent DDM data, we simulate several instances of a gaze-based DDM and fit the resulting data with various constrained versions of the non-gaze-based DDM. We also analyze two empirical eye-tracking datasets that exhibit gaze-dependent behavior and show how a non-gaze based DDM fit to those data can similarly produce a variety of value-dependent parameters. In sum, we show how not accounting for gaze-dependent mechanisms can lead to particular patterns in drift variability, boundary separation, or processing/motor time based on OV. This highlights the importance of accounting for gaze when analyzing decision-making data.

1.1. The standard DDM

In the DDM (Ratcliff, 1978; Ratcliff & McKoon, 2008), decisions are made when option information accumulated from a starting point z, reaches one of two boundaries, 0 or a. The drift rate of the accumulation process, v, indexes the rate at which evidence is acquired. In value-based two-alternative forced-choice tasks (2AFC), this parameter represents the relative difference in strength of preference between the two options. Processes outside of the evidence accumulation are represented by the non-decision time parameter T_{er}. The starting point z is assumed to vary from trial-to-trial and is drawn from a uniform distribution with range sz. Non-decision time is also assumed to have a uniformly distributed trial-to-trial variability with range st. Furthermore, the trial-to-trial standard deviation in drift rate is expressed by the parameter η. The model also assumes that there is random variation in the evidence from one moment to another. The standard deviation of this variation, s, is typically fixed to 0.1 or 1 to serve as a scaling parameter, since the units of evidence in the model are arbitrary.

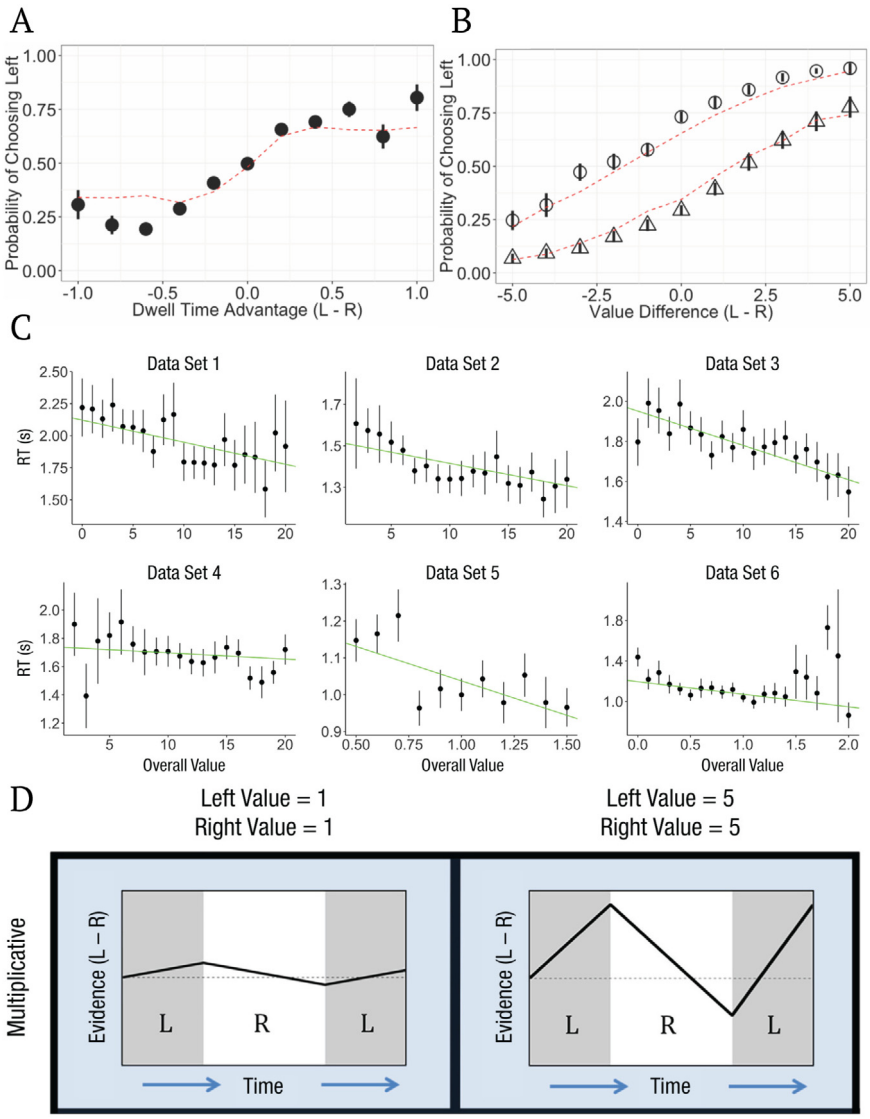

Fig. 1. Features of multiplicative-gaze DDMs. The effect of relative gaze time (A) and last fixation (B) on choice in data analyzed in Smith and Krajbich (2018). The probability of choosing an option increases the longer it is gazed at and when it is fixated on last. In these panels, (A-B) points are empirical data, (B) open circles represent trials where the left option was fixated on last, open triangles represent trials where the right option was fixated on last, error bars show standard errors of the mean across subjects, and (A-B) red dashed lines represent predictions from a multiplicative-gaze model. (C) The relationship between overall value and RT in the six datasets analyzed in Smith et al. (2019). In these panels, the black points are data points and error bars show standard errors of the mean across subjects. Green lines are linear regressions fitted to the data, very similar to those generated by multiplicative-gaze models. (D) Illustration of the multiplicative effect of gaze on the decision process. In this model, gaze alternates between the left (L) and right (R) options. The magnitude of the effect of gaze shifts on accumulated evidence is greater for higher OVs (here 1 vs. 1 compared to 5 vs. 5). Reprinted with permission from Smith and Krajbich (2018), Smith et al. (2019). . (For interpretation of the references to color in this figure legend, the reader is referred to the web version of this article.)

Usually, researchers parameterize the DDM such that the boundary separation and starting point are determined before the beginning of the decision. In other words, these parameters do not depend on stimulus properties. This means that under usual assumptions, these parameters should not vary with OV. In some cases, relaxing these assumptions have led to better model fits. Therefore, in the following analyses we bin the data into different conditions based on OV and estimate parameters separately across these conditions.

1.2. Multiplicative-gaze DDMs

Multiplicative-gaze models like the aDDM (Krajbich et al., 2010) similarly view 2AFC as involving a noisy evidence accumulation process with two boundaries. The primary difference between this model and the standard DDM is that, in the aDDM, the drift rate changes depending on gaze location. In the standard DDM one can model the drift rate towards the more valuable option as a function of the two option values:

$$v = d \times \left| r_{left} - r_{right} \right| \quad (1)$$

where r_{left} and r_{right} represent the stimulus values of the options on the left- and right-hand side of the screen, and d is a scaling parameter to account for the units of r. In the aDDM, this function has an additional parameter θ that discounts the value of the non-fixated option.[1] More specifically, there are two drift rates, depending on gaze location:

[1] Unlike the standard DDM, the aDDM typically holds the boundary separation parameter constant, and instead estimates the standard deviation of the noise in the diffusion process.

$$v = \begin{cases} d \times \left(r_{left} - \theta r_{right}\right) \text{ if gaze left} \\ d \times \left(\theta r_{left} - r_{right}\right) \text{ if gaze right.} \end{cases} \quad (2)$$

Since θ multiplies the non-fixated item's value, the gaze-dependent shifts in drift rate depend on OV. To illustrate this effect, assume r_{Left} and r_{right} are both set to 1, $d = 0.5$, and $\theta = 0.3$:

$$v = d \times \left(r_{left} - \theta r_{right}\right) = 0.5 \times (1 - (0.3 \times 1)) = 0.35$$
$$v = d \times \left(\theta r_{left} - r_{right}\right) = 0.5 \times ((0.3 \times 1) - 1) = -0.35$$

However, if r_{Left} and r_{right} are both set to 5 (using the same values for d and θ):

$$v = d \times \left(r_{left} - \theta r_{right}\right) = 0.5 \times (5 - (0.3 \times 5)) = 1.75$$
$$v = d \times \left(\theta r_{left} - r_{right}\right) = 0.5 \times ((0.3 \times 5) - 5) = -1.75$$

On average, the decision process will terminate more quickly in the latter case, due to the increased variability in the drift rate (Fig. 1D).

2. Simulation study

In this section we report the results of a series of simulation studies evaluating how a conventional DDM would recover parameters from data generated with a multiplicative-gaze model. Our goal was to gauge how DDMs with the assumption that drift rates are invariant to OV would accommodate data generated from a multiplicative-gaze model, which integrates gaze-weighted values into the drift-rate formulation (Eq. (2)).

2.1. General procedure

The general procedure to perform this parameter recovery exercise was as follows:

1. Generate a single set of group-level parameters x_{gen}^{Group}.
2. Generate multiple sets of subject-level parameters x_{gen}^{Subj}.
3. Simulate an 'experimental' dataset D using the aDDM.
4. Generate a set of fitted group-level parameters $x_{fit-DDM}^{Group}$ using different versions of the DDM.

The experimental paradigm simulated here is a 2AFC task between options given *a priori* subjective value ratings (Krajbich et al., 2010). We assume that each option is given a value rating on a scale from 0–10, and that decision-makers are motivated to choose the option with a higher value.

2.1.1. Parameter generation

We used a hierarchical approach to generating parameters. At the group-level, each set of parameters x_{gen}^{Group} was sampled from a uniform distribution using ranges that roughly matched parameter values reported in the literature (Smith et al., 2019):

$$\mu_d \in \mathcal{U}(0.0002, 0.0004)$$
$$\mu_s \in \mathcal{U}(0.02, 0.03)$$
$$\mu_\theta \in \mathcal{U}(0.1, 0.9)$$
$$\mu_{Ter} \in \mathcal{U}(350, 650).$$

Next, we generated 40 sets of subject-level parameters x_{gen}^{Subj} based on the initial set of group-level parameters. These subject-level parameters were sampled from normal distributions:

$$d_i \in \mathcal{N}(\mu_d, \sigma_d^2)$$
$$s_i \in \mathcal{N}(\mu_s, \sigma_s^2)$$
$$\theta_i \in \mathcal{N}(\mu_\theta, \sigma_\theta^2)$$
$$Ter_i \in \mathcal{FN}(\mu_{Ter}, \sigma_{Ter}^2),$$

Table 1
Values used to simulate data.

Value-Difference (VD) condition	Overall-Value (OV) condition	Values
Easy (VD = 3)	Low value (OV = 3)	{0, 3}
Easy (VD = 3)	Medium value (OV = 10)	{3.5, 6.5}
Easy (VD = 3)	High value (OV = 17)	{7, 10}
Moderate (VD = 2)	Low value (OV = 3)	{0.5, 2.5}
Moderate (VD = 2)	Medium value (OV = 10)	{4, 6}
Moderate (VD = 2)	High value (OV = 17)	{7.5, 9.5}
Hard (VD = 1)	Low value (OV = 3)	{1, 2}
Hard (VD = 1)	Medium value (OV = 10)	{4.5, 5.5}
Hard (VD = 1)	High value (OV = 17)	{8, 9}

where each 'experimental' dataset used a slightly different set of standard deviation (σ^2) parameters. See Table S1 in the Supplementary Materials for x_{gen}^{Group} used in each simulation study.

2.1.2. Data generation

We generated datasets using the aDDM with a temporal resolution of 1 ms. Typically, models with multiplicative-gaze, such as the aDDM, are fit using empirical gaze data (Krajbich et al., 2010). For these simulations, we randomly sampled gaze durations from a uniform distribution: $\mathcal{U}(0.5 \times gaze_{median}, 1.5 \times gaze_{median})$. All simulated datasets were generated using median gaze durations of 500 ms.

For each simulated dataset D, data were generated using each of the 40 subject-level parameter sets x_{gen}^{Subj}. Each subject's data consisted of nine conditions: three levels of value difference {1,2,3}, and for each of those, three levels of OV {low, medium, high}. The specific values for each condition can be found in Table 1. We generated 1000 trials for each condition. For each trial, option values were randomly assigned to the left and right locations, and the first fixation location was determined by trial number: even-numbered trials started with a left fixation, and odd-numbered trials started with a right fixation. Subsequent fixations alternated between the two locations until a decision was made.

We selected a subset of 100 trials per condition for our subsequent analyses. This subset was selected to improve the comparability between the simulation studies and empirical studies because the latter had fewer trials per condition. Ultimately, the results of our model fitting exercises were consistent regardless of the sample size we used (see Table S2 in the Supplementary Materials for additional details).

2.1.3. DDM model fitting

We fit eight different versions of the non-gaze based DDM to choice outcomes and RT distributions within each condition. Here, we only considered models where the drift rate varied with the value-difference (e.g., Krajbich et al., 2010; Milosavljevic et al., 2010). Drift rates are held invariant to OV due to the nature of evidence accumulation in these models. In the DDM, evidence accumulation reflects the relative difference between options along some feature like subjective value; therefore, only value differences are thought to matter during the decision process (Ratcliff & McKoon, 2008; Ratcliff, Voskuilen, Teodorescu, 2018). As such, in each of these models, the drift rate parameter (v) was assumed to be constant across OV conditions and was only allowed to vary with value-difference. The other parameters (i.e., a, T_{er}, and η) were either held constant or allowed to vary across conditions (Table 2). To allow for a wide range of possible inferences, we included versions of the model where different combinations of the free parameters were allowed to vary across OV conditions.

Table 2
Description of the models fit to simulated datasets.

Model	Free parameters	Constant across OV	Constant across all conditions	Fixed parameters
Model 1	a, T_{er}, η	v	–	z, s
Model 2	T_{er}, η	v	a	z, s
Model 3	a, η	v	T_{er}	z, s
Model 4	a, T_{er}	v	η	z, s
Model 5	η	v	a, T_{er}	z, s
Model 6	T_{er}	v	a, η	z, s
Model 7	a	v	T_{er}, η	z, s
Model 8	s	v	η, T_{er}	z, a

Note: Free parameters were estimated independently per OV condition. Fixed parameters were not estimated from the data. "a" stands for boundary separation, "T_{er}" for non-decision time, "η" for across-trial noise in drift rate, "v" for drift rate, "z" for starting point, and "s" for within-trial diffusion noise.

We considered one additional model. Most variations of the DDM keep within-trial variability constant while freely estimating boundary separation (a). In contrast, studies using the aDDM have held a constant while freely estimating s. Therefore, we considered a model where boundary separation was held constant, and s was allowed to vary by OV condition. This model (Model 8) resembles the σ Model presented by Ratcliff, Voskuilen, Teodorescu (2018), where within-trial diffusion noise was estimated as a function of overall magnitude.

All models were estimated using the HDDM toolbox (Wiecki, Sofer, & Frank, 2013). HDDM uses Markov chain Monte Carlo sampling to approximate group and individual parameters within a hierarchical Bayesian framework. For all models, we report the mean posterior estimate and 95% highest density interval (HDI). All models were fit using 2 chains of 15 000 samples each with 5000 burn-in samples. We performed model comparisons using DIC (Spiegelhalter, Best, Carlin, & Linde, 2002) and BPIC (Ando, 2007) scores. While DIC scores are available in the HDDM package, we include BPIC scores as a more conservative test when accounting for model complexity (i.e., including additional model parameters).

For Models 1–7, we used a standard fitting approach where $s = 1$. Model 8 was calculated by transforming the parameters from Model 7, which estimated a in each OV condition. Since Model 8 holds boundary separation constant, we used the average of the posterior samples of the a parameter ($\bar{a}$) across OV conditions in Model 7. To make this transformation, we first divided $\bar{a}$ by the posterior samples of each a parameter (i.e., a_{Low}, a_{Medium}, a_{High}) to calculate separate rescaling factors (F_{OV}) for each OV condition:

$$F_{OV} = \bar{a}/a_{OV}. \quad (3)$$

For each OV condition, within-trial diffusion noise was calculated using the following equation:

$$\text{transformed } S_{OV} = F_{OV}. \quad (4)$$

Similarly, we rescaled v and η by multiplying each posterior sample of these parameters in a given OV condition by the respective rescaling factor F_{OV}, and then taking average of those rescaled sample estimates.

2.2. Simulation Study 1

2.2.1. Data generation

For Simulation Study 1, we used the data-generating process detailed in Section 2.1.2. When sampling the 40 subject-level parameters x_{gen}^{Subj}, we used the following standard deviations:

$$\sigma_d^2 = 0.00001$$
$$\sigma_s^2 = 0.001$$
$$\sigma_\theta^2 = 0.01$$
$$\sigma_{Ter}^2 = 10.$$

Here, we chose conservative values to minimize variability for this first simulation study. In subsequent studies, we used more liberal values to allow for more across-subject variability. The group-level means for this and all subsequent studies are detailed in Table S1 in the Supplementary Materials.

Table 3
Simulation study 1 model comparison.

Model	Free parameters	# of parameters	DIC	BPIC
Model 1	a, T_{er}, η	12	100 268	100 278
Model 2	ter, η	10	100 641	100 964
Model 3	a, η	10	100 294	100 303
Model 4	a, T_{er}	10	**100 266**	**100 278**
Model 5	η	8	100 684	100 691
Model 6	T_{er}	8	101 093	101 101
Model 7	a	8	100 295	100 303
Model 8	s	8	100 295	100 303

Note: "a" stands for boundary separation, "T_{er}" for non-decision time, "η" for across-trial noise in drift rate, "v" for drift rate, "z" for starting point, and "s" for within-trial diffusion noise.

2.2.2. Model fitting results

The results of Simulation Study 1 are summarized in Table 3 and Fig. 2. The best fitting model estimated separate a and T_{er} parameters in each OV condition (Model 4). For the standard DDM (with s fixed), only models which allowed a to vary (i.e., Models 1, 3, 4, and 7) were able to produce posterior predictions that approximate the patterns found in the simulated data (Fig. 2A). These qualitative patterns can be mostly fit by varying just the a parameter (i.e., Model 7: Fig. 2B). Although these models overestimate accuracy rates in the High OV condition, the RT patterns are well-captured at all but the slowest RT quantiles. In these models, the fitted a estimates were smaller in higher OV conditions ($\mu_{a\text{Low}} = 2.05$ [95% HDI: 2.05, 2.06]; $\mu_{a\text{Mid}} = 1.93$ [95% HDI: 1.92, 1.93]; $\mu_{a\text{High}} = 1.73$ [95% HDI: 1.73, 1.74]). In other words, these models tell us that boundary separation is decreasing with OV, even though we know that the generating model held boundaries constant. Moreover, the approximately 16% difference between $\mu_{a\text{Low}}$ and $\mu_{a\text{High}}$ is similar to that found in empirical studies (e.g., Cavanagh et al., 2014; Pirrone, Azab et al., 2018; Pirrone, Wen et al., 2018).

Models that allowed η to vary and not a (i.e., Models 2, 5, and 8) were able to capture the RT patterns, but grossly underestimate the accuracy in the High OV conditions (Fig. 2C). In these models, the fitted η values were larger for higher OVs ($\mu_{\eta\text{Low}} = 0.01$ [95% HDI: 3×10^{-4}, 0.03]; $\mu_{\eta\text{Mid}} = 0.28$ [95% HDI: 0.24, 0.31]; $\mu_{\eta\text{High}} = 1.25$ [95% HDI: 1.23, 1.28]). These models tell us that across-trial variability in drift rate is increasing with OV. This interpretation is accurate, but the gazed-based model goes a step further, allowing us to attribute some of the noise to gaze effects.

Models that allowed T_{er} to vary and not a (i.e., Models 2 and 6) could not account for the differences in accuracy across OV conditions (see Fig. 2D). Moreover, these models mostly capture the differences between the fastest RT quantiles (Q.1) and miss the increased spread between OV conditions in the slower quantiles. In these models, the fitted T_{er} values were smaller for higher OVs ($\mu_{Ter\text{Low}} = 0.43$ [95% HDI: 0.43, 0.44]; $\mu_{Ter\text{Mid}} = 0.42$ [95% HDI: 0.42, 0.42]; $\mu_{Ter\text{High}} = 0.39$ [95% HDI: 0.39, 0.39]). These models tell us that non-decision time is decreasing with OV, which we know was not the case in the model that generated the data.

The only other model that captured the patterns found in the simulated data was Model 8, which held a constant, while allowing s to vary. Within this model, s increased with OV ($\mu_{s\text{Low}} =$

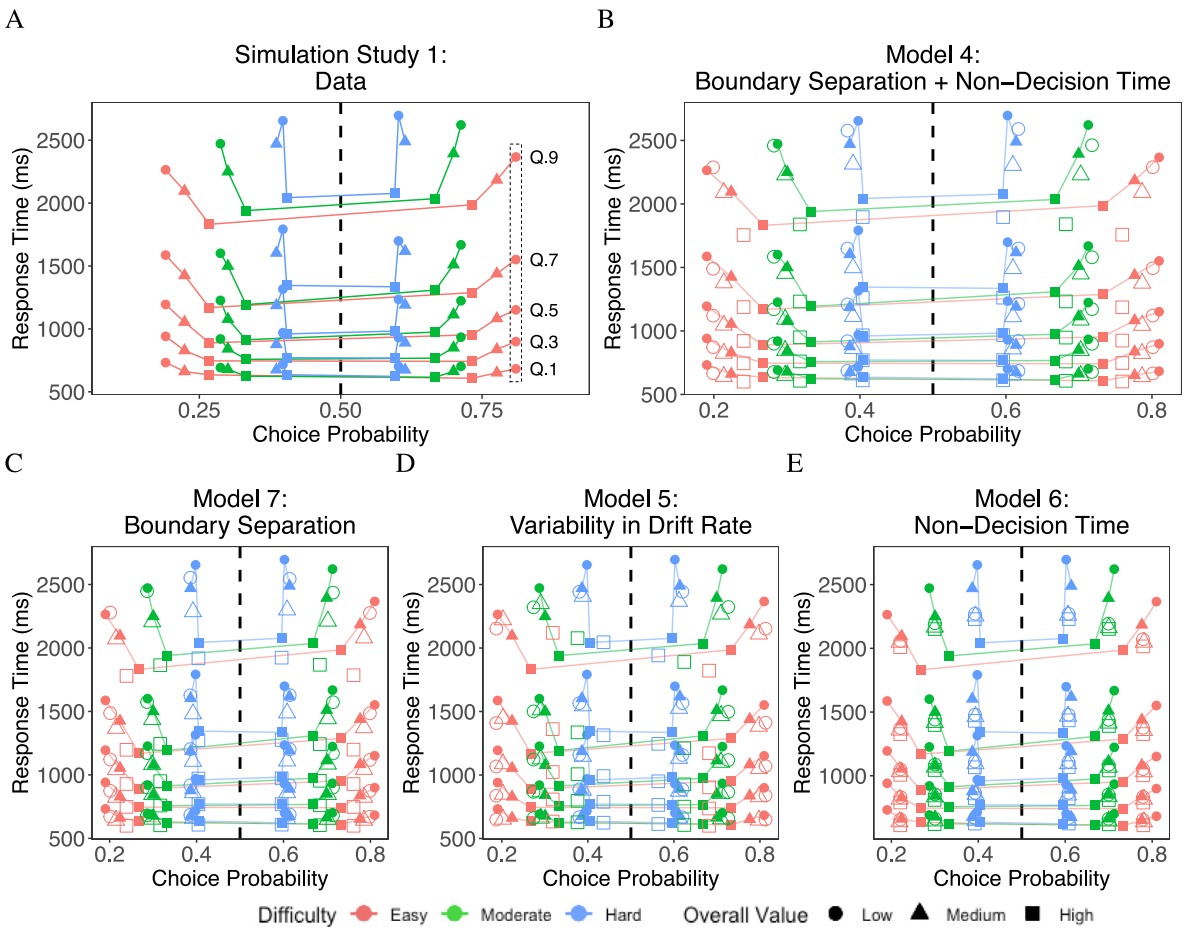

Fig. 2. Quantile-probability (Q-P) plots for (A) data from Simulation Study 1 and (B-E) predictions from exemplar DDM models. Shapes represent the overall value (OV) of a condition (circle: OV = 3; triangle: OV = 10; square: OV = 17), while colors represent the difficulty (value difference; VD) of the condition (red: VD = 3; green: VD = 2; blue: VD = 1). For each condition, we plot the response time (RT) quantiles for correct (choice probability above 0.5) and error responses (choice probability below 0.5). Q.9, Q.7, Q.5, Q.3, Q.1 represent the 90%, 70%, 50%, 30%, and 10% quantiles of the RT distributions, respectively. (A) Simulation Study 1 data (100 trials per condition). If responses were invariant towards OV, we would expect responses within a VD condition to have the same accuracy and RT regardless of the OV condition. Instead, the simulated data show that within a given difficulty condition, the correct and error responses display a U-shaped pattern, where accuracy and RT decrease with OV. (B) Posterior-predictive data (open shapes) from Model 4, where boundary separation (a) and non-decision time (T_{er}) vary by OV condition, fit to simulated data from Panel A (solid shapes). (C) Posterior-predictive data from Model 7, where boundary separation (a) alone varies by OV condition. (D) Posterior-predictive data from Model 5, where across-trial variability in drift rates (η) alone varies by OV condition (E) Posterior-predictive data from Model 6, where non-decision time (T_{er}) alone varies by OV condition. For other models, see Supplementary Figures S1-7. . (For interpretation of the references to color in this figure legend, the reader is referred to the web version of this article.)

0.93 [95% HDI: 0.93, 0.93]; $\mu_{sMid} = 0.99$ [95% HDI: 0.98, 0.99]; $\mu_{sHigh} = 1.10$ [95% HDI: 1.10, 1.10]). The interpretation is that OV increases the within-trial noise in the decision process. Again, this is not entirely inaccurate, but the source of the variability is not explicitly attributed to gaze.

2.2.3. Discussion

The results of this simulation study provide preliminary evidence, showing fits of the DDM can yield various explanations for a behavioral phenomenon when relaxing common assumptions about boundary separation and non-decision time. If the DDM were fit holding variability in drift rate constant across OV conditions, a likely conclusion would be that OV affects boundary separation. If instead boundary separation was held constant as a function of stimulus properties, as is often assumed, then the conclusion would be that OV affects non-decision time.

2.3. Simulation Study 2

2.3.1. Data generation

For Simulation Study 2, we used the same group-level parameters x_{gen}^{Group} as were generated in Simulation Study 1. However, when sampling the 40 subject-level parameters x_{gen}^{Subj}, we used the following standard deviations:

$$\sigma_d^2 = 0.0001$$
$$\sigma_s^2 = 0.01$$
$$\sigma_\theta^2 = 0.1$$
$$\sigma_{Ter}^2 = 100.$$

Here, we chose liberal values to maximize inter-subject variability for this simulation study.

2.3.2. Results

The results of Simulation Study 2 are summarized in Table 4 and Fig. 3. Similar to Simulation Study 1, the best fitting model estimated separate a and T_{er} parameters in each OV condition. (i.e., Model 4). Once again, the versions of the DDM which best capture the qualitative patterns in the simulated data were those that allowed the a parameter to vary with OV. The models that varied the η parameter with OV produced posterior predictions that could not differentiate between the Low OV and Medium OV conditions, and underestimated the accuracy of High OV conditions (Fig. 3C), while the models that varied the T_{er} could not

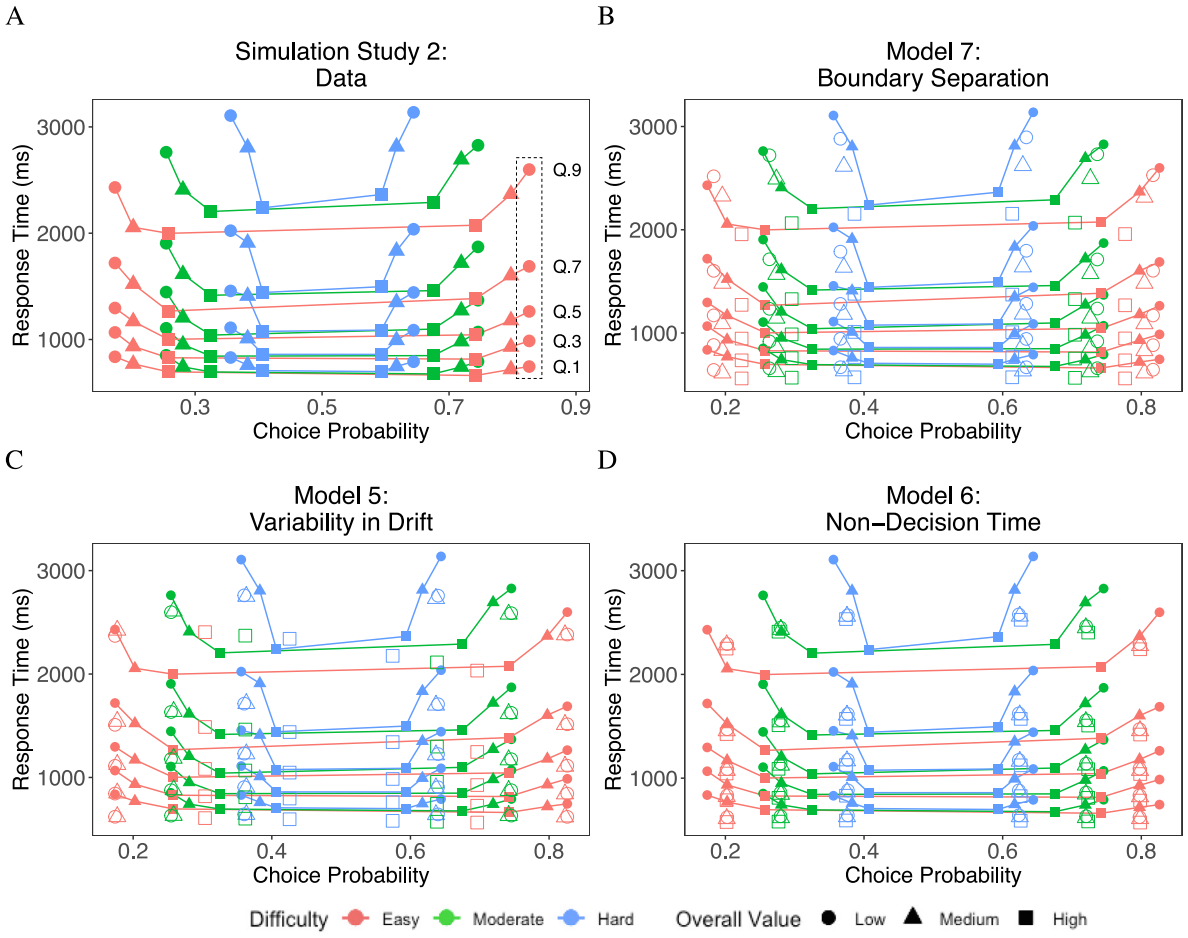

Fig. 3. Quantile-probability (Q-P) plots for (A) data from Simulation Study 2 and (B-D) predictions from exemplar DDM models. Shapes represent the overall value (OV) of a condition (circle: OV = 3; triangle: OV = 10; square: OV = 17), while colors represent the difficulty (value difference; VD) of the condition (red: VD = 3; green: VD = 2; blue: VD = 1). For each condition, we plot the response time (RT) quantiles for correct (choice probability above 0.5) and error responses (choice probability below 0.5). Q.9, Q.7, Q.5, Q.3, Q.1 represent the 90%, 70%, 50%, 30%, and 10% quantiles of the RT distributions, respectively. (A) Simulation Study 2 data (100 trials per condition). (B) Posterior-predictive data (open shapes) from Model 7, where boundary separation (a) alone varies by OV condition, fit to simulated data (solid shapes). (C) Posterior-predictive data from Model 5, where across-trial variability in drift rates (η) alone varies by OV condition (D) Posterior-predictive data from Model 6, where non-decision time (T_{er}) alone varies by OV condition. . (For interpretation of the references to color in this figure legend, the reader is referred to the web version of this article.)

differentiate between any of the conditions (Fig. 3D). Although the model that varied the a parameter with OV slightly underestimated RTs and overestimated the High OV condition's accuracy, this model produced predictions that could easily distinguish the different conditions (Fig. 3B).

2.3.3. Discussion

We show that models that vary the boundary separation with OV can capture the basic patterns of data generated with attention-based processes, even when there was increased inter-subject variability across multiple decision parameters.

2.4. Simulation Studies 3–4

To confirm the results discussed above, we generated two more simulated datasets using liberal standards for parameter variability with different sets of group-level parameters.

2.4.1. Data generation

For Simulation Studies 3–4, we used identical procedures to Simulation Study 2. The only difference was that we sampled a new set of group level parameter values for each study.

Table 4
Simulation study 2 model comparison.

Model	Free parameters	# of parameters	DIC	BPIC
Model 1	a, T_{er}, η	12	114 087	114 097
Model 2	ter, η	10	114 395	114 404
Model 3	a, η	10	114 168	114 177
Model 4	a, T_{er}	10	**114 084**	**114 094**
Model 5	η	8	114 409	114 416
Model 6	T_{er}	8	114 949	114 956
Model 7	a	8	114 168	114 175
Model 8	s	8	114 168	114 175

Note: "a" stands for boundary separation, "T_{er}" for non-decision time, "η" for across-trial noise in drift rate, "v" for drift rate, "z" for starting point, and "s" for within-trial diffusion noise.

2.4.2. Results

The results of Simulation Study 3 and Simulation Study 4 are summarized in Table 5 and Fig. 4. Similar to the previous simulation studies, the best fitting model in both Simulation Study 3 and Stimulation Study 4 estimated separate a and T_{er} parameters in each OV condition (i.e., Model 4). Models that allow a to vary with OV could capture the qualitative order of RTs and accuracy rates found in the simulations. However, these models'

Table 5
Simulation studies 3 and 4 model comparison.

Model	Free parameters	# of parameters	Simulation Study 3		Simulation Study 4	
			DIC	BPIC	DIC	BPIC
Model 1	a, T_{er}, η	12	146 256	146 266	126 911	126 921
Model 2	ter, η	10	146 673	146 682	127 125	127 133
Model 3	a, η	10	146 430	146 439	126 924	126 932
Model 4	a, T_{er}	10	**146 253**	**146 263**	**126 908**	**126 918**
Model 5	η	8	146 732	146 739	127 144	127 150
Model 6	T_{er}	8	148 256	148 264	127 196	127 203
Model 7	a	8	146 560	146 467	126 921	126 928
Model 8	s	8	146 560	146 467	126 921	126 928

Note: "a" stands for boundary separation, "T_{er}" for non-decision time, "η" for across-trial noise in drift rate, "v" for drift rate, "z" for starting point, and "s" for within-trial diffusion noise.

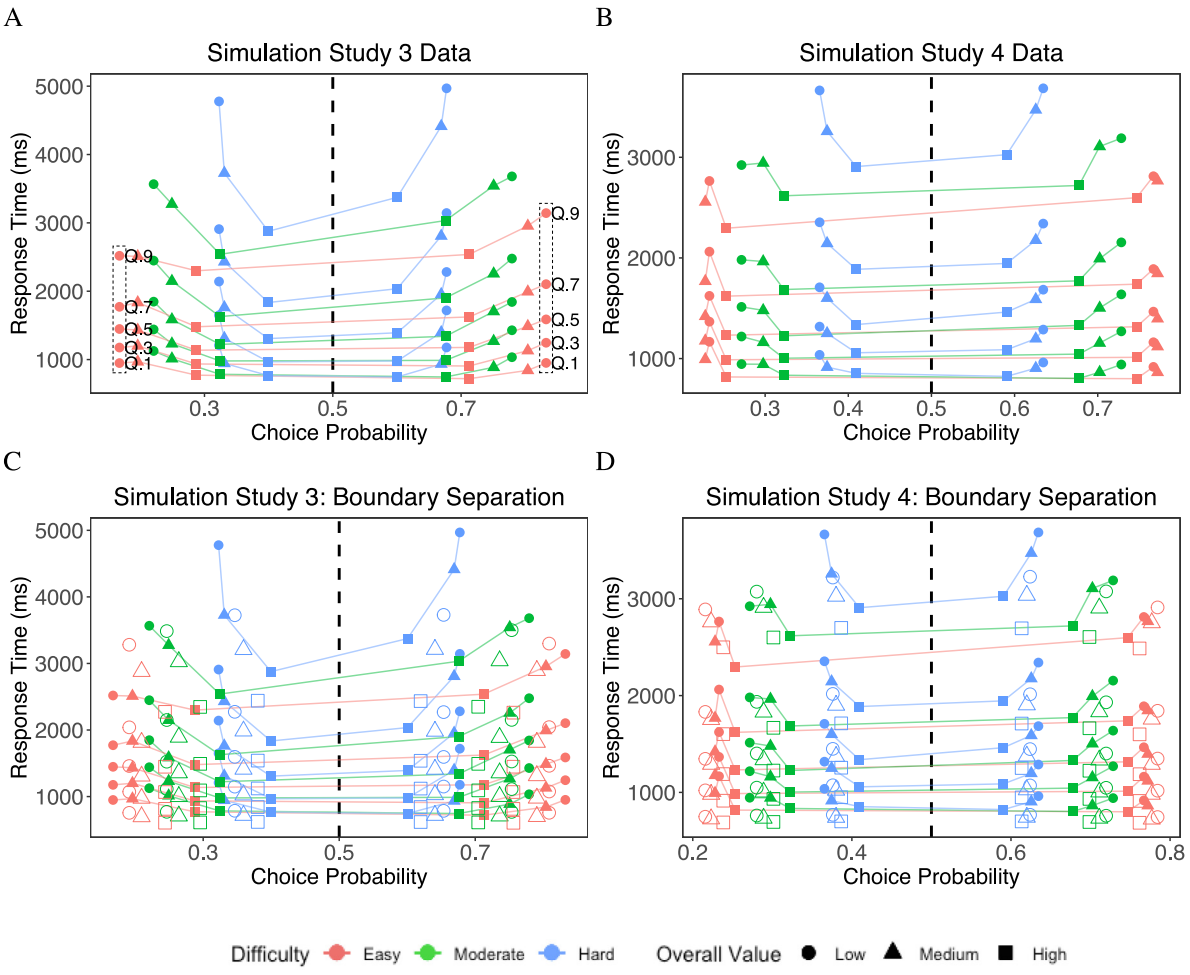

Fig. 4. Quantile-probability (Q-P) plots for data from (A) Simulation Study 3 and (B) Simulation Study 4 data (100 trials per condition). Shapes represent the overall value (OV) of a condition (circle: OV = 3; triangle: OV = 10; square: OV = 17), while colors represent the difficulty (value difference; VD) of the condition (red: VD = 3; green: VD = 2; blue: VD = 1). For each condition, we plot the response time (RT) quantiles for correct (choice probability above 0.5) and error responses (choice probability below 0.5). (C, D) Posterior-predictive data (open shapes) from Model 7, where boundary separation (a) alone varies by OV condition, fit to simulated data (solid shapes). . (For interpretation of the references to color in this figure legend, the reader is referred to the web version of this article.)

posterior predictions were less reliable in capturing the large accuracy difference between the conditions in Simulation Study 3.

2.4.3. Discussion

We confirm that conventional versions of the DDM will identify boundary separation as the mechanism responsible for generating the OV effect. Although these models capture the basic behavioral patterns, they miss certain features in the data, such as the negative correlation between accuracy and OV.

2.5. Simulation Study 5–8

For Simulation Studies 5–8, we explored the robustness of the previous results by examining data generated under a variety of circumstances. When generating each dataset, we limited the inter-subject variability for all but a single parameter. For Simulation Studies 5–8 we evaluated the impact of more variability in the drift rate scaling (d) parameter, within-trial variability (s) parameter, attention (θ) parameter, and non-decision time (T_{er}) parameter relative to the other parameters, respectively.

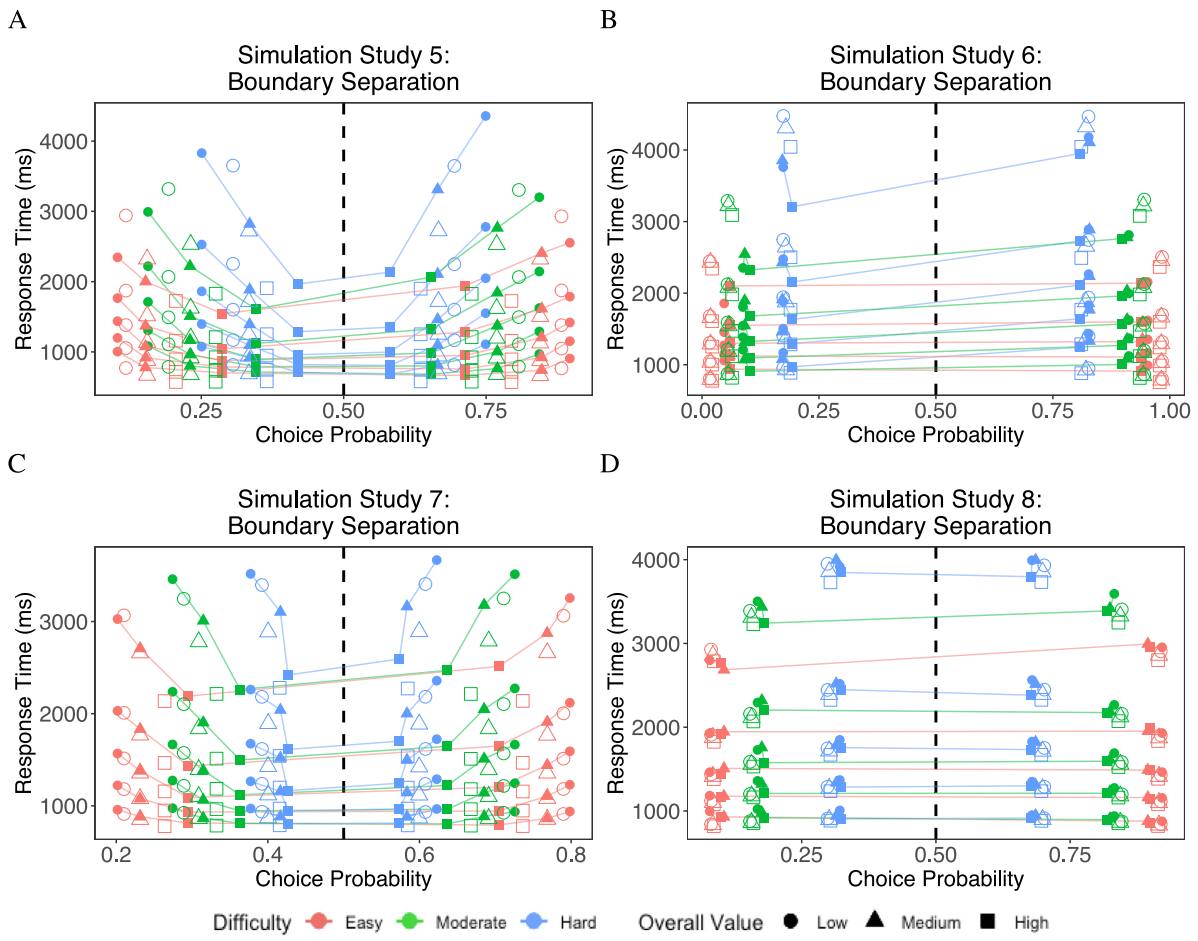

Fig. 5. Quantile-probability (Q-P) plots for (A) Simulation Study 5, (B) Simulation Study 6, (C) Simulation Study 7, and (D) Simulation Study 8 (100 trials per condition). Posterior-predictive data (open shapes) from Model 7, where boundary separation (a) alone varies by OV condition, fit to simulated data (solid shapes). Shapes represent the overall value (OV) of a condition (circle: OV = 3; triangle: OV = 10; square: OV = 17), while colors represent the difficulty (value difference; VD) of the condition (red: VD = 3; green: VD = 2; blue: VD = 1). For each condition, we plot the response time (RT) quantiles for correct (choice probability above 0.5) and error responses (choice probability below 0.5). . (For interpretation of the references to color in this figure legend, the reader is referred to the web version of this article.)

Table 6
Simulation studies 5–8 model comparison.

Model	Simulation Study 5		Simulation Study 6		Simulation Study 7		Simulation Study 8	
	DIC	BPIC	DIC	BPIC	DIC	BPIC	DIC	BPIC
Model 1	**110 918**	**110 928**	117 142	117 152	123 959	123 969	111 174	111 184
Model 2	111 834	111 184	117 524	117 534	123 976	123 984	111 225	111 323
Model 3	111 158	111 167	117 162	117 170	123 955	123 964	111 173	111 181
Model 4	111 178	111 187	**117 138**	**117 147**	123 956	123 966	111 172	111 181
Model 5	112 118	112 125	117 610	117 618	123 982	123 988	111 290	111 296
Model 6	115 386	115 393	118 708	118 715	123 973	123 981	111 221	111 229
Model 7	111 582	111 589	117 160	117 167	**123 953**	**123 960**	**111 170**	**111 177**
Model 8	111 582	111 589	117 160	117 167	**123 953**	**123 960**	**111 170**	**111 177**

Note: "a" stands for boundary separation, "T_{er}" for non-decision time, "η" for across-trial noise in drift rate, "v" for drift rate, "z" for starting point, and "s" for within-trial diffusion noise.

2.5.1. Data generation

For each simulation study, we used the procedures outlined in Section 2.1.2 to generate a unique set of group-level parameters x_{gen}^{Group}. When sampling the subject-level parameters x_{gen}^{Subj}, we used the conservative standard deviations from Simulation Study 1 for all parameters except d (Simulation Study 5: $\sigma_d^2 = 0.0001$), s (Simulation Study 6: $\sigma_s^2 = 0.01$), θ (Simulation Study 7: $\sigma_\theta^2 = 0.1$), or T_{er} (Simulation Study 8: $\sigma_{Ter}^2 = 100$).

2.5.2. Results

The results of Simulation Studies 5–8 are summarized in Table 6 and Fig. 5. The best fitting model in Simulation Study 5 estimated separate a, T_{er}, and η parameters in each OV condition (i.e., Model 1). In Simulation Study 6, the best fitting model estimated separate a and T_{er} parameters in each condition (i.e., Model 4). In Simulation Studies 7 and 8, the best fitting models estimated separate a parameters in each condition (i.e., Model 7).

2.5.3. Discussion

Interestingly, the most complicated model best fit the data in Simulation Study 5. Evidently the across-trial variability parameter (η) in the DDM was needed to account for the extra variation in the drift rate scaling parameter (d). However, all datasets were best fit with models that allowed boundary separation to vary with OV.

3. Empirical study

The goal of this section is twofold: first, we show patterns in empirical data (Cavanagh et al., 2014; Smith & Krajbich, 2018) that demonstrate the OV effect; second, we examine DDM fits to that data, to see whether patterns in the parameter values correspond to what we saw in the simulation studies. We find that value-dependent boundary separation, non-decision time, and drift-rate variability all improve model fit.

3.1. Method

3.1.1. Dataset 1

In this reinforcement learning study (Cavanagh et al., 2014), participants ($N = 20$) initially learned three stimulus pairings with the following probabilities of being the correct choice: A:B (80%:20%), C:D (70%:30%), and E:F (60%:40%). Each stimulus was a unique Japanese Hiragana character. Participants went through this training phase until they reached a minimum criterion of choosing the better stimulus in each pair. Participants then proceeded to the testing phase where they chose between all possible pairings for 240 trials across two sessions.

We classified each trial according to the OV of the stimuli in the trial: low value trials containing only low probability stimuli (20%, 30%, or 40%), high value trials containing only high probability stimuli (60%, 70%, or 80%), or mixed value trials containing one low value stimulus and one high value stimulus.

We excluded trials with excessively fast (slow) decisions, less (more) than 2 standard deviations below (above) participant-level means, using log(RT). Such trials are likely to have been terminated due to accidental button presses, intentional skipping, or distraction. Using these criteria, we excluded 3.7% of trials.

3.1.2. Dataset 2

Participants ($N = 44$) in this study (Smith & Krajbich, 2018) first rated 147 food items on a scale from −10 to 10 before making 200 choices between positively rated items (rating > 0). Although participants in this study completed three other choice tasks (200 trials each), we only focus on the food choice data.[2] Food items were selected such that no item was used in more than 7 trials and the maximum absolute rating difference was 5. Some participants ($n = 22$) did not have a sufficient number of positively rated food items to generate 200 valid trials, so these participants completed as many trials as could satisfy the constraints ($M = 171.3$ trials). Participants earned a $5 show-up fee, additional money from the other tasks, and a food chosen from one random trial.

We classified each trial according to the OV of the food items in the trial. Low value trials were those where both food items were less than the median value (5.5), high value trials were those where both items were greater than the median value, and mixed value trials were those with one low and one high value item. We excluded participants ($n = 20$) with less than 10 trials in any of the three conditions. We also excluded one participant whose mean RT (3.39 s) was 60% slower than the group mean excluding that participant (1.43 s). Furthermore, we excluded trials with excessively fast (slow) decisions, less (more) than 2 standard deviations below (above) participant-level means, using log(RT). Using these criteria, we excluded 4.3% of trials.

[2] The other tasks involved multiple attributes/stimuli per option, and thus require additional assumptions about how subjective value is calculated.

Table 7
Description of the models fit to empirical datasets.

Model	Varies with OV	Constant across conditions	Drift rate (v) formulation	Fixed parameters
DDM 1	–	a, T_{er}	Eq. (5)	η, z
DDM 2	a	T_{er}	Eq. (5)	η, z
DDM 3	T_{er}	a	Eq. (5)	η, z
DDM 4	η	a, T_{er}	Eq. (5)	z

Note: Free parameters were estimated independently per OV condition. Fixed parameters were not estimated from the data. "v" for drift rate, "a" stands for boundary separation, "T_{er}" for non-decision time, "η" for across-trial noise in drift rate, and "z" for starting point.

3.2. Analyses

We fit the DDMs to choice outcomes and RT distributions using the procedures outlined in Section 2.1.3. We estimated four different versions of the DDM. Once again, the drift rate parameter (v) was assumed to be constant across OV conditions; it was only allowed to vary with trial-level value-difference:

$$v \sim v_{Intercept} + v_{Dif}(r_{left} - r_{right}), \tag{5}$$

where r_{left} and r_{right} refer to the value of the left and right options, respectively. Additionally, the starting-point parameter was set to $z = a \times 0.5$. The other parameters (i.e., a, T_{er}, and η) were either held constant or allowed to vary across conditions (Table 7).

All models were estimated using the HDDM toolbox (Wiecki et al., 2013). For all models, we report the mean posterior estimate and 95% highest density interval (HDI). All models were fit using 2 chains of 15 000 samples each with 5000 burn-in samples.

We performed model comparisons using DIC (Spiegelhalter et al., 2002) and BPIC (Ando, 2007) scores. To statistically test the difference in parameter values, we report Bayes Factors to quantify the strength of evidence for or against the null hypothesis using the Savage–Dickey density ratio (Wagenmakers, Lodewyckx, Kuriyal, & Grasman, 2010).

We conducted posterior predictive checks to assess the predictive accuracy of each model. From each model we sampled 100 sets of parameter values from the posterior distributions and simulated a dataset for each participant using those parameters. For each sample, we binned participants' trials into groups based on value difference and overall value (Dataset 1: 9 groups; Dataset 2: 12 groups). We then separated the trial bins into correct and error responses and calculated RT quantiles for each. This posterior data was then compared to that of the empirical data.

3.3. Results

3.3.1. Behavioral results

What are the behavioral markers of OV? Fig. 6 illustrates some of these effects in the two empirical datasets. In Dataset 1 (panel A), High OV trials (squares) were slightly less accurate than both Low OV (circles) and Mixed OV (triangles) trials. Additionally, both error and correct responses in High OV trials (squares) were much faster than their Low OV and Mixed OV counterparts across the RT quantiles in both hard (blue) and moderate (green) contexts. Notably, correct responses in both hard and moderate High OV trials were almost as fast as those in the easy, Mixed OV trials.

Similarly, Dataset 2's (panel B) correct responses in High OV trials were also faster than in the Low OV trials for most RT

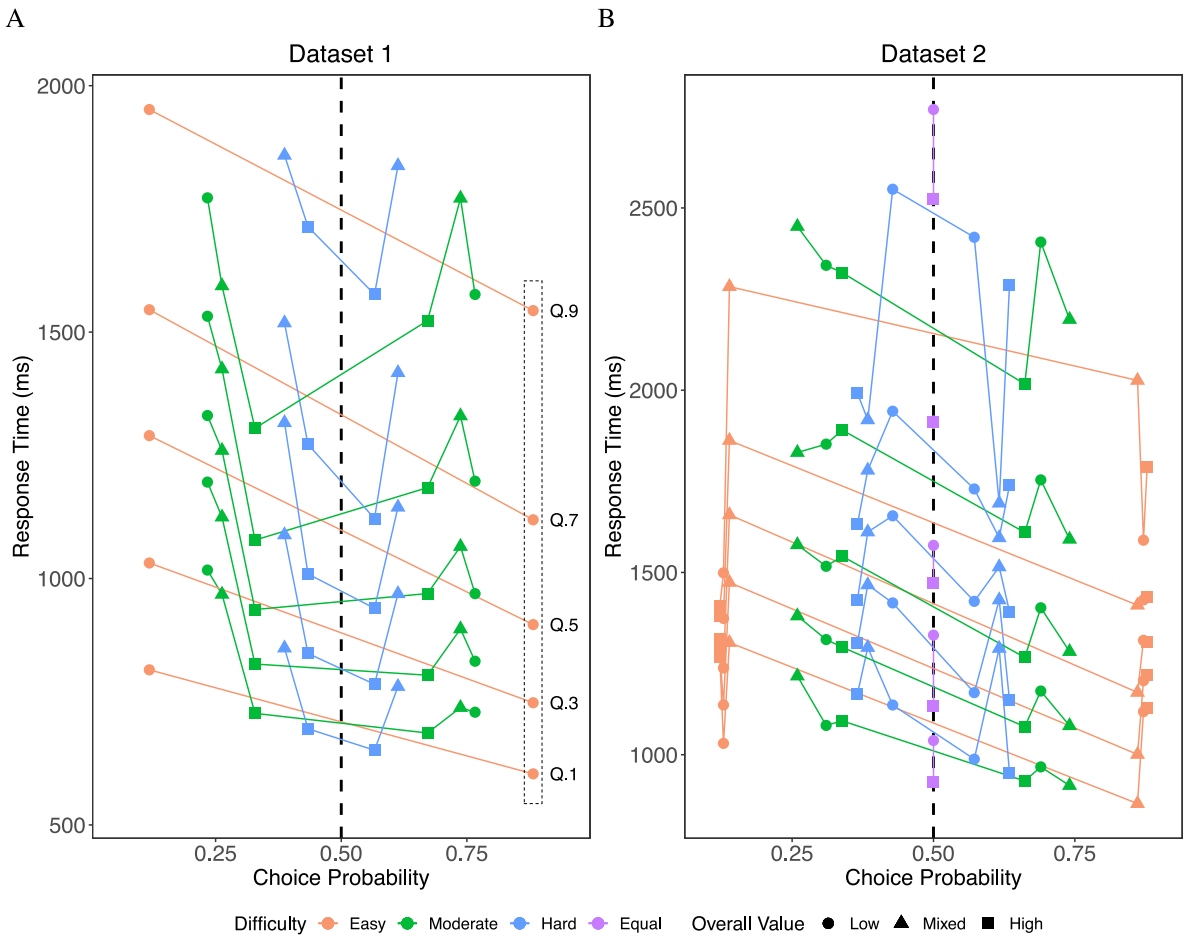

Fig. 6. Empirical choice behavior by OV. Panels show the relationship among RT-conditioned choice accuracy (i.e., the probability of choosing the better option), value, and difficulty. Shapes represent the overall value (OV) of a condition (circle: low OV; triangle: mixed OV; square: high OV), while colors represent the difficulty (value difference; VD) of the condition (red: easy conditions; green: moderate conditions; blue: hard conditions; purple: equal value conditions). For each condition, we plot the response time (RT) quantiles for correct choice (choice probability above 0.5). Q.9, Q.7, Q.5, Q.3, Q.1 represent the 90%, 70%, 50%, 30%, and 10% quantiles of the RT distributions, respectively. Panel **(A)** is based on choice and RT behavior from Dataset 1 (Cavanagh et al., 2014), where value represents probability of winning. Panel **(B)** is from Dataset 2 (Smith & Krajbich, 2018), where value represents subjective value ratings on a scale from 1 to 10. . (For interpretation of the references to color in this figure legend, the reader is referred to the web version of this article.)

quantiles regardless of difficulty. Correct responses in the High OV trials were also faster than Mixed OV trials across difficulty levels, except for the fasted RT quantile (Q.1) in the moderate difficulty condition and the two slowest RT quantiles (Q.7, Q.9) in the hard difficulty condition. Additionally, the relationship among RTs between these conditions was less consistent for error responses.

While the High OV trials had the lowest accuracy in Dataset 1, this was more variable in Dataset 2. In the latter data, High OV trials were more accurate than Low OV trials for hard conditions, but less accurate in moderate conditions. Accuracy was higher in Mixed OV trials than High OV trials for both difficulty conditions.

Overall, the empirical data from Dataset 1 reasonably resemble the data from the simulation studies. When excluding the Mixed OV trials, OV decreases both accuracy and RT, generating a U-shaped pattern among conditions with the same difficulty in the QP plots. In contrast, the empirical data from Dataset 2 demonstrate cases where OV *increases* accuracy while decreasing RT. And while OV had mostly symmetrical effects on correct and error responses in both the simulation studies and Dataset 1 (ignoring Mixed OV), there is noticeable asymmetry between the RTs of correct and error responses in Dataset 2. Moreover, Dataset 2 exhibits somewhat different patterns at fast and slow quantiles, at least for hard decisions.

In summary, these qualitative patterns suggest that OV is primarily impacting the RT distribution, rather than accuracy rates. Correct responses in High OV trials were almost always faster than in Low OV trials. However, High OV accuracy was sometimes higher and sometimes lower than in Low OV trials, depending on the difficulty of the condition (quantitative analyses of both accuracy and RT can be found in the Supplementary Materials).

3.3.2. *Model fitting results*

To evaluate whether variable boundaries significantly improved the DDM, we compared model fits using the deviance information criterion (DIC; Spiegelhalter et al., 2002) and the Bayesian predictive information criterion (BPIC; Ando, 2007; see Table 8).

Dataset 1 was best fit by a model where boundary separation varied with OV (DDM 2). In contrast, Dataset 2 was best fit by the non-decision time variant (DDM 3). According to the former model (DDM 2), response caution is decreasing with OV. The latter model (DDM 3) indicates that basic encoding and/or motor responses are becoming faster with OV.

We followed up these analyses with Bayesian hypothesis testing on the parameters that were estimated separately for each OV condition among these best fitting models. We ran three sets of tests, comparing the difference between parameter estimates in (1) High OV and Low OV trials; (2) High OV and Mixed OV

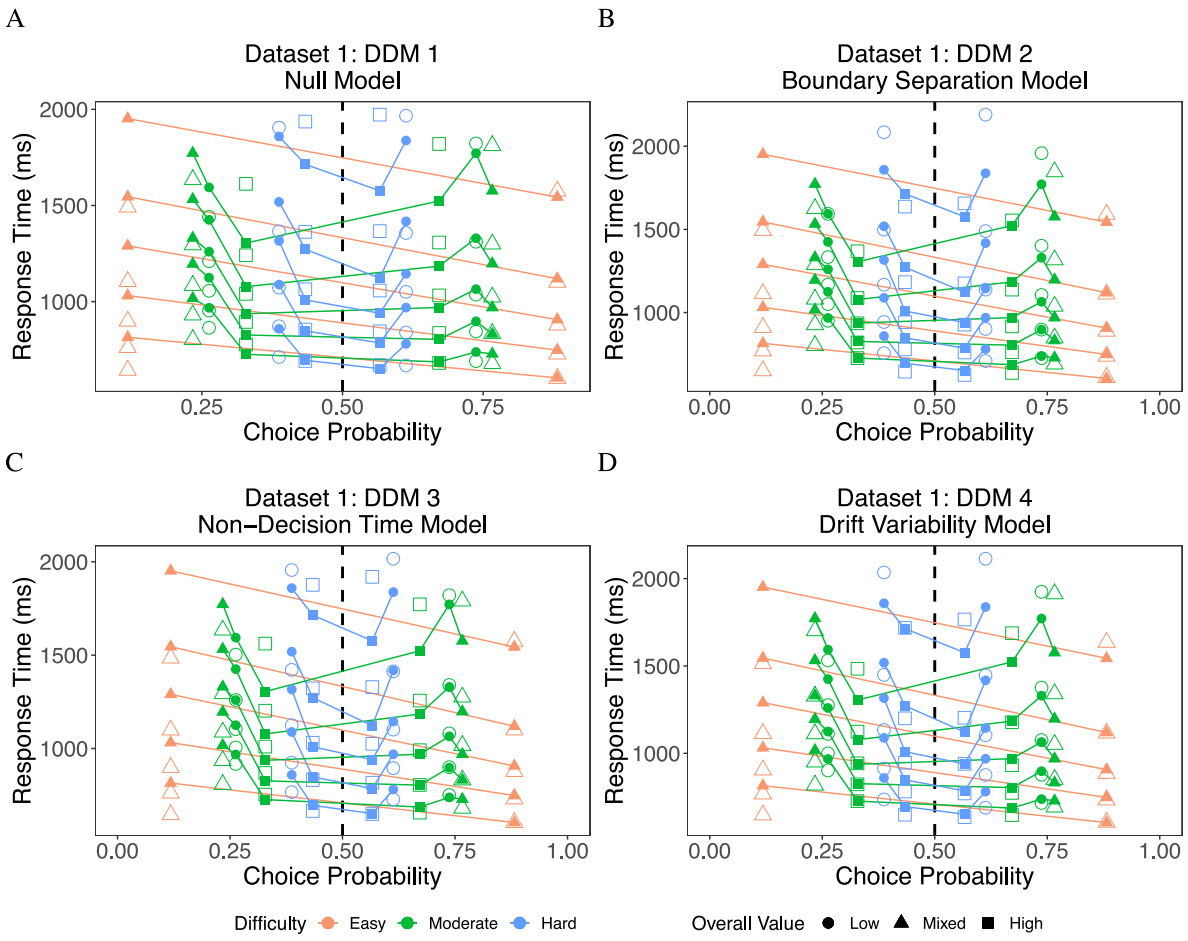

Fig. 7. Quantile-probability plots for the DDM fit to Dataset 1. The plots display the empirical (solid shapes) and posterior-predictive (open shapes) response proportion and RT quantiles for choosing the correct (right side of 0.50) and error (left side of 0.50) option. Shapes represent the overall value (OV) of a condition (circle: Low OV; triangle: Mixed OV; square: High OV), while colors represent the difficulty (value difference; VD) of the condition (red: easy conditions; green: moderate conditions; blue: hard conditions). (A) The standard DDM alone does not reproduce the OV effect on RTs. (B) Adding value-dependent boundaries allows the model to generate the OV effect on RT but exaggerates the difference between the High OV and Low OV conditions, especially at slower RT quantiles (Q.7, Q.9). (C) Value-dependent non-decision time generates the OV effect with smaller differences between the High and Low OV conditions but does worse at capturing the error RTs. (D) Value-dependent across-trial variability generates similar predictions as the boundary-separation model but underestimates the difference in RTs between the Mixed OV and Low OV conditions. . (For interpretation of the references to color in this figure legend, the reader is referred to the web version of this article.)

Table 8
Model fit indices of the models fit to empirical data.

Model 1	OV-dependent parameter	DDM	
		DIC	BPIC
Dataset 1	–	8472	8525
Dataset 2	–	9232	9283
Model 2			
Dataset 1	a	**8366**	**8452**
Dataset 2	a	9196	9279
Model 3			
Dataset 1	T_{er}	8386	8464
Dataset 2	T_{er}	**9173**	**9251**
Model 4			
Dataset 1	η	8400	8454
Dataset 2	η	9206	9260

Note. Here, "a" stands for boundary separation, "T_{er}" for non-decision time, and "η" for across-trial variability in drift. Bold font indicates best fitting model. See Table S83 in the Supplementary Materials for additional details.

trials; and (3) Mixed OV and Low OV trials. As detailed in Section *3.2*, we report Bayes Factors (BF) from the Savage–Dickey density ratio test favoring the null hypothesis. For these tests, BF values above 1 represent support for the null hypothesis that parameters are equal between OV conditions, while BF values below 1 represent support for the alternative hypothesis that parameters differ between conditions.

For Dataset 1, we found strong evidence that boundary separation was reduced in the High OV trials compared to the Low OV trials (DDM 2: BF = 0.162). There was strong evidence against a difference between the Mixed OV and Low OV boundaries (DDM 2: BF = 6.813), and very weak evidence that boundaries in the High OV trials were reduced compared to the Mixed OV trials (DDM 2: BF = 0.800).

For Dataset 2, we found weak evidence that Low OV had longer non-decision time compared to both High OV (DDM 3: BF = 0.442) and Mixed OV conditions (DDM 3: BF = 0.697). Additionally, we found weak evidence against a difference between the High OV and Mixed OV trials (DDM 3: BF = 1.590).

Next, we turn to posterior predictive checks. We checked whether the various models could correctly predict the mean accuracy of each condition, as well as the RT quantiles for correct and error responses. As can be seen in Fig. 7, the DDM is unable to predict the observed pattern of fast High OV correct and error responses in Dataset 1, unless value-dependent parameters are added. The posterior predictive check for Dataset 2 was more

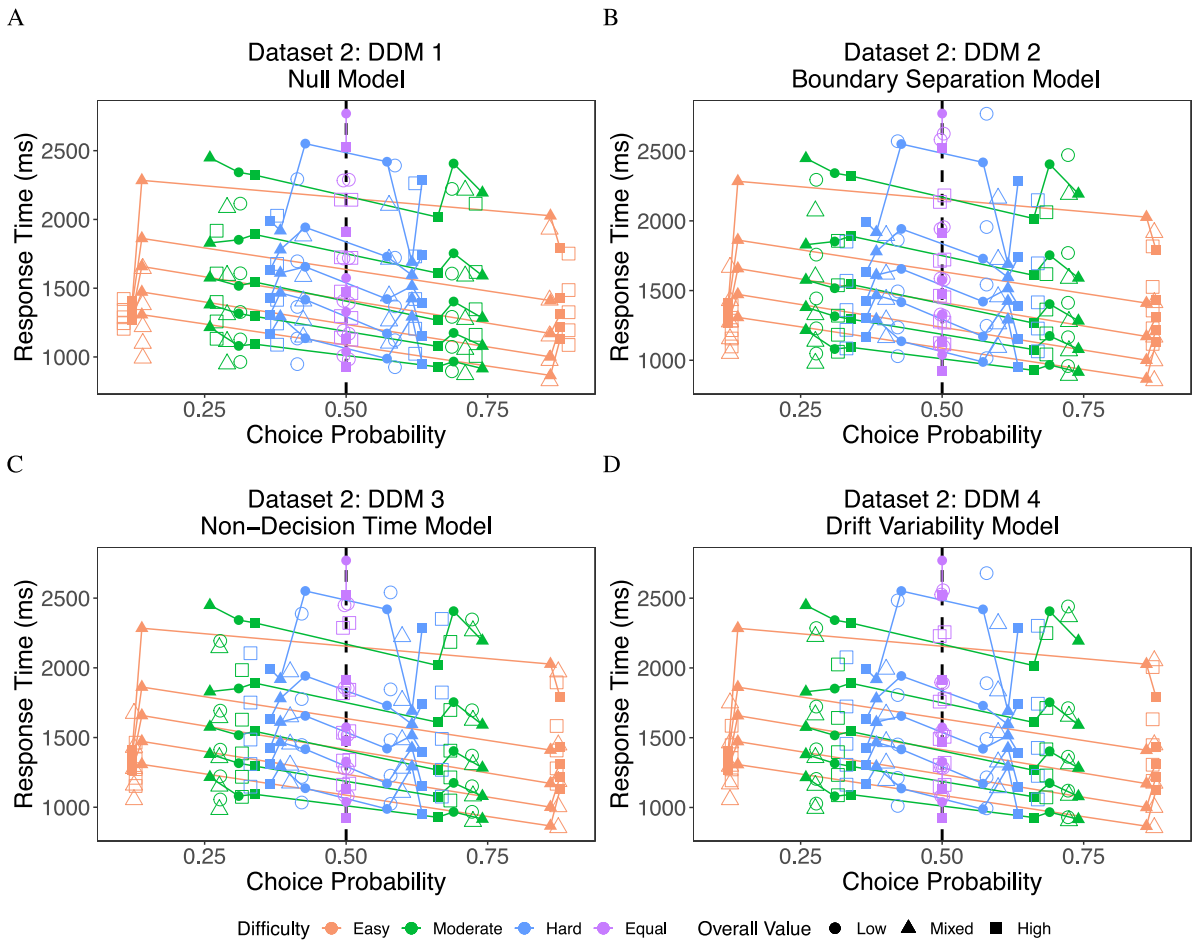

Fig. 8. Quantile-probability plots for the DDM fit to Dataset 2. The plots display the empirical (solid shapes) and posterior-predictive (open shapes) response proportion and RT quantiles for choosing the correct (right side of 0.50) and error (left side of 0.50) option. Shapes represent the overall value (OV) of a condition (circle: Low OV; triangle: Mixed OV; square: High OV), while colors represent the difficulty (value difference; VD) of the condition (red: easy conditions; green: moderate conditions; blue: hard conditions; purple: equal value conditions). (A) The standard DDM only produces the OV effect in the slowest RT quantiles, and only in the Moderate and Hard difficulty conditions. Adding value-dependent boundaries (B), non-decision time (C), or drift variability (D) allows the model to generate the OV effect for additional RT quantiles. However, each of these models exhibits substantial bias. . (For interpretation of the references to color in this figure legend, the reader is referred to the web version of this article.)

ambiguous. As can be seen in Fig. 8, none of the models can reliably produce the OV effect in all RT quantiles.

Overall, we found that several different model parameters could account for the OV effect in empirical data. In these models, boundary separation and/or non-decision time appeared to decrease in the High OV trials.

4. Discussion

Empirically, increases in overall value (OV) result in shorter decision times. Recent research has argued that this OV effect is due to gaze amplification of value during the decision process (Smith et al., 2019), but there are other explanations that involve drift rate variability or boundary separation. Here, we demonstrated patterns in DDM parameters that can result from fitting the DDM to data generated from a gaze-based DDM. In particular, we observe drift-rate variability that increases with OV, decision boundaries that decrease with OV, or non-decision times that decrease with OV. We also observed similar patterns in two empirical datasets.

When it comes to computational modeling, researchers can take a variety of approaches when adjusting model parameters to capture behavioral phenomena such as the OV effect. However, with each approach comes an implicit assumption about the latent cognitive mechanisms. Throughout our analyses, we focused on boundary separation and non-decision time because these are parameters that other studies have allowed to vary with OV (e.g., Cavanagh et al., 2014; Fontanesi et al., 2019; Pirrone, Azab et al., 2018; Pirrone, Wen et al., 2018; Ratcliff & Frank, 2012). Alternatively, one can allow within-trial noise in the diffusion process or across-trial drift-rate-variability parameters to account for OV (Bose et al., 2020; Brunton et al., 2013; Kvam & Pleskac, 2016; Ratcliff, Voskuilen and McKoon, 2018; Ratcliff, Voskuilen, Teodorescu, 2018; Teodorescu et al., 2016). We see the variability models as less conceptually different from the gaze-based models because they are simply less specific about the source of noise in the decision process. Moreover, there may be additional sources of drift-rate variability beyond attention. In contrast, diffusion models that condition boundary separation or non-decision time on OV offer a very different interpretation.

In the gaze-dependent DDMs, the latent mechanism underlying the OV effect is gaze-driven information gain. In the aDDM, this is implemented through the θ parameter, which discounts the subjective value of unlooked-at options (Krajbich et al., 2010; Smith et al., 2019). We used models with multiplicative-gaze as our default mechanism for the OV effect for the simple reason that these models also explain gaze-dependent effects on choice (Smith et al., 2019). Over the past decade there have been a number of papers documenting the relationship between attention and choice (see Krajbich, 2019), including domains such as

consumer/food choice (Fisher, 2017; Folke, Jacobsen, Fleming, & De Martino, 2016; Gluth, Kern, Kortmann, & Vitali, 2020; Krajbich et al., 2010; Sepulveda et al., 2020; Sullivan, Hutcherson, Harris, & Rangel, 2015; Towal et al., 2013), risky choice (Glickman et al., 2019; Gluth, Spektor, & Rieskamp, 2018; Johnson & Busemeyer, 2016; Stewart, Hermens and Matthews, 2016), intertemporal choice (Amasino et al., 2019; Stewart, Chater, & Brown, 2006), social preferences (Ashby et al., 2016; Smith et al., 2019; Stewart, Gächter, Noguchi and Mullett, 2016), aesthetic choice (Vaidya & Fellows, 2015), moral preferences (Fiedler & Glöckner, 2015; Pärnamets et al., 2015), and reinforcement learning (Cavanagh, Malalasekera, Miranda, Hunt, & Kennerley, 2019; Cavanagh et al., 2014; Konovalov & Krajbich, 2020). Moreover, support for gaze-based DDMs have also been found in the brain. Researchers have found correlations between gaze-dependent value signals and activity in value-sensitive regions such as the ventromedial prefrontal cortex and ventral striatum (Hunt et al., 2018; Lim, O'Doherty, & Rangel, 2011). And neurophysiological research with monkeys has found that visually attending to an appetitive cue increased neural firing in the orbitofrontal cortex (McGinty, 2019; McGinty, Rangel, & Newsome, 2016). Thus, we believe that it is vital to consider attention when trying to account for the OV effect.

Our analysis of the empirical data would have been strengthened by directly comparing the DDM with a gaze-contingent model such as the aDDM. Unfortunately, a proper comparison is not possible due to limitations of current fitting methods in estimating models with time-dependent drift rates. Yet it is this very mechanism that generates the OV effect in gaze-contingent models. However, when we approximate the aDDM with a single drift rate, the model can partially accommodate the OV effects (see Smith et al., 2019). When fit to the empirical data, these models produce qualitative patterns that resemble the non-gaze models reported in this paper, but with lower DIC/BPIC scores. This suggests that multiplicative-gaze models can do as good of a job, if not better, than models without multiplicative-gaze.

One unanswered question is whether it would be problematic to fit a gaze-based model to data generated from a non-gaze based DDM with varying noise or boundaries. Even without eye-tracking data, a multiplicative-gaze model could be fit to the choice-conditioned RT distributions. If there were OV effects in the RTs (e.g., due to value-dependent boundaries), this would presumably lead to such a model to be fit with significant gaze effects. We did not address this possibility here because every study using multiplicative-gaze models has established a link between gaze and choice before fitting the model. For example, the aDDM's attentional discounting parameter (θ) can be estimated directly from the relationship between gaze proportions, option value, and choice probability (Smith et al., 2019), providing an alternative validation for the RT-based estimates. Therefore, any fits of a gaze-based model without eye-tracking data would need to be interpreted with caution.

Interestingly, the work by Cavanagh et al. (2014) did incorporate eye-tracking data yet found value-dependent boundaries. However, the researchers focused on an alternative formulation for how attention influences drift rate, namely, an additive effect that is constant regardless of the option values. This model does not generate the OV effect and so does not address the issues raised in this paper.

Cavanagh et al. (2014) also linked changing boundary separation to changes in pupil diameter. While this provides an interesting new link between the DDM and biological measures, it does not by itself confirm that boundaries are changing with OV. It could be the case that pupil dilation simply reflects OV. Neuroimaging studies have found that brain activity does reflect OV, suggesting that this statistic is either represented or at least correlated with some computation that is represented in the brain (Frömer & Shenhav, 2019; Hunt et al., 2012).

Our analyses in the simulation study found that any model that estimated boundary separation separately for each condition was able to qualitatively capture the patterns found in the simulated data. Additionally, the best fitting model was one where both boundary separation and non-decision time were estimated separately for different OV conditions. However, the data generating process included gaze-weighted drift rates and not variable boundary separation or non-decision time. We therefore advise caution in interpreting decision boundaries or non-decision times that vary with OV without also considering attention during the value comparison process. More generally, we caution against letting boundary separation or non-decision time vary based on trial-level features, because what looks like evidence for varying boundaries may simply be unaccounted-for drift-rate effects.

Overall-value-sensitive boundary separation can capture the observed behavior because decreasing boundaries reduce RTs while slightly decreasing accuracy. However, accuracy sometimes increased with OV in the empirical data, which decreasing boundaries alone cannot accommodate. Moreover, this explanation requires decision-makers to somehow adjust their decision boundaries each trial based on OV. According to joint neural-cognitive computational modeling, information signaling conflict in the anterior cingulate cortex amplify subthalamic conflict responses, adjusting boundary separation through pathways separate from those that accumulate noisy value signals (Botvinick et al., 2001; Cavanagh et al., 2011; Ratcliff & Frank, 2012; Shenhav et al., 2013; Vassena et al., 2020). These conflict signals could function as a warning, indicating the need for more deliberation (Cavanagh et al., 2011, 2014; Ratcliff & Frank, 2012). In contrast, models of cognitive control allow for ad-hoc adjustments to boundary separation during high-difficulty contexts to facilitate more timely responses (Botvinick et al., 2001; Shenhav et al., 2013; Vassena et al., 2020). In either case, it remains unclear why this conflict-mediated pathway would result in increased boundary separation in Low OV trials relative to High OV trials. In fact, Cavanagh et al. (2014) argue that a cautionary mechanism is needed to prevent impulsive responses when high values are present. Adjusting decision boundaries trial-by-trial also seems cognitively costly to the small, debatable advantage that it conveys in terms of accuracy and RT. It also challenges the norms of diffusion modeling, where the decision boundaries are typically set prior to stimulus presentation and are constant within an experimental condition (Ratcliff & McKoon, 2008).

On the other hand, OV-sensitive non-decision time is an unlikely explanation for the observed behavior. Non-decision time, representing time spent encoding information and/or executing a response, primarily sets the floor for the fastest responses within a condition (i.e., the first RT quantile), shifting all RTs by a fixed amount, and should have no effect on accuracy (Ratcliff & Smith, 2004; Ratcliff & Tuerlinckx, 2002). The OV effect is almost absent in the fastest RT quantiles, strongest in the slowest RT quantiles, and has inconsistent but appreciable effects on accuracy. This suggests that OV has an effect throughout the course of the decision process in a manner inconsistent with a non-decision-time explanation.

In contrast, OV-sensitive noise parameters are more established in the DDM literature. Researchers have developed diffusion models where stimulus magnitudes are used to calculate the noise in the decision process in auditory discrimination tasks (Brunton et al., 2013), brightness discrimination tasks (Ratcliff, Voskuilen, Teodorescu, 2018; Teodorescu et al., 2016), numerosity magnitude estimation tasks (Ratcliff & McKoon, 2018), and motion discrimination tasks (Ratcliff, Voskuilen, McKoon, 2018). Additionally, the notion that perceptual noise increases in relation to magnitude is well established in psychophysics, going

back to Fechner in 1860 (see Ratcliff, Voskuilen, Teodorescu, 2018 for a more thorough discussion of the history of magnitude-sensitive noise in the psychophysics literature). However, despite the theoretical appeal of DDMs with noise that increase with OV, our paper shows that such assumptions may not be necessary once one accounts for the role of gaze in two-alternative, value-based choice. Nonetheless, additional research is still needed to determine whether attention plays a comparable role in the perceptual tasks discussed above. Although the aDDM was designed for value-based tasks, it has been successfully applied to perceptual decisions, such as angle estimation (Tavares et al., 2017) and numerosity discrimination (Sepulveda et al., 2020). We conjecture that the analysis of attention can offer insights into magnitude effects in domains outside of two-alternative, value-based tasks.

For these reasons, we recommend that researchers reassess previously reported associations between OV and boundary separation, non-decision time, or noise parameters (Fontanesi et al., 2019; Green, Biele, & Heekeren, 2012; Pirrone, Azab et al., 2018; Pirrone, Wen et al., 2018; Ratcliff & Frank, 2012; Ratcliff, Voskuilen, McKoon, 2018; Teodorescu et al., 2016). In some cases, this reassessment will not dramatically alter the conclusions of the study. For example, Fontanesi et al. (2019) used value-dependent boundaries out of convenience to account for the magnitude effects' asymmetrical effect on RTs and accuracy rates, and the authors made no further attempts to interpret these patterns. In other cases, this reassessment will be more impactful. For example, Pirrone, Azab et al. (2018) and Pirrone, Wen et al. (2018) concluded that the observation of value-dependent boundaries was evidence of an adaptive decision policy that incorporates speed-value trade-offs. Teodorescu et al. (2016) offered a similar argument, connecting magnitude-based noise parameters to a bottom-up speed-value trade-off. Green et al. (2012) found that boundary separation decreased with higher rewards in a perceptual task and linked those changes to effective connectivity between cortico-striatal and cerebellar-striatal brain systems. Considering that gaze-dependent effects in our simulation study were captured by changes in boundary separation, non-decision time, and/or noise parameters, revisiting these experiments with eye-tracking is necessary to determine whether these parameters were accurately capturing OV effects.

We also recommend that researchers account for OV effects in experimental designs that include value-based, binary choice tasks. While previous research has carefully controlled for value differences between conditions, these studies have often ignored how OV may differ across conditions and affect parameter estimates (Amasino et al., 2019; Cavanagh et al., 2011; Chen & Krajbich, 2018; De Martino, Fleming, Garrett, & Dolan, 2013; Diederich, 2003; Dutilh & Rieskamp, 2016; Hare, Schultz, Camerer, O'Doherty, & Rangel, 2011; Helfer & Shultz, 2014; Konovalov & Krajbich, 2019; Merkel & Lohse, 2019; Milosavljevic et al., 2010; Philiastides & Ratcliff, 2013; Pisauro, Fouragnan, Retzler, & Philiastides, 2017; Rodriguez, Turner, & McClure, 2014; Shenhav, Straccia, Cohen, & Botvinick, 2014). Although we cannot be certain about how gaze-dependent drift rates would alter the results in these studies, our current results suggest that several DDM parameters can be sensitive to OV effects. For example, Milosavljevic et al. (2010) observed that high time pressure decreased boundary separation and increased noise in the drift rate. While those are the expected results of applying time pressure, any imbalance in the number of high-value trials between conditions could also have contributed to those effects.

As an aside, another limitation of DDM fits is that parameter estimates, especially for across-trial variability parameters, tend to be biased in small datasets (Boehm et al., 2018; Lerche, Voss, & Nagler, 2017; van Ravenzwaaij, Donkin, & Vandekerckhove, 2017). However, using hierarchical Bayesian estimation procedures like HDDM is known to increase the reliability of parameter estimates, even in smaller datasets (Boehm et al., 2018; Lerche et al., 2017; Ratcliff & Childers, 2015).

In theory, multiplicative-gaze models could account for effects that otherwise manifest as noise in model fits. In the standard DDM, external noise can enter into the evidence accumulation process through either within-trial fluctuations or across-trial variability (Ratcliff, Voskuilen, McKoon, 2018; Ratcliff, Voskuilen, Teodorescu, 2018). If gaze patterns were identical across-trials, then shifts in gaze at the trial-level would contribute to within-trial fluctuations, while if gaze patterns were different across trials, that would additionally contribute to across-trial variability. We would further expect that value would be more highly discounted when it is more difficult to divide attention between options (e.g., when stimuli are widely separated on a display). However, additional work is needed to specify the exact relationship between gaze patterns and these noise parameters.

Acknowledgments

This research was funded by Career Award 1554837 from the National Science Foundation and the Cattel Sabbatical Fund.

Appendix A. Supplementary data

Supplementary material related to this article can be found online at https://doi.org/10.1016/j.jmp.2021.102594.

References

Amasino, D. R., Sullivan, N. J., Kranton, R. E., & Huettel, S. A. (2019). Amount and time exert independent influences on intertemporal choice. *Nature Human Behaviour*, *3*(4), 383–392. http://dx.doi.org/10.1038/s41562-019-0537-2.

Ando, T. (2007). Bayesian predictive information criterion for the evaluation of hierarchical Bayesian and empirical Bayes models. *Biometrika*, *94*(2), 443–458. http://dx.doi.org/10.1093/biomet/asm017.

Armel, K. C., Beaumel, A., & Rangel, A. (2008). Biasing simple choices by manipulating relative visual attention. *Judgment and Decision Making*, *3*(5), 396–403.

Ashby, N. J. S., Jekel, M., Dickert, S., & Glöckner, A. (2016). Finding the right fit: A comparison of process assumptions underlying popular drift-diffusion models. *Journal of Experimental Psychology: Learning, Memory, and Cognition*, *42*(12), 1982–1993. http://dx.doi.org/10.1037/xlm0000279.

Boehm, U., Annis, J., Frank, M. J., Hawkins, G. E., Heathcote, A., Kellen, D., et al. (2018). Estimating across-trial variability parameters of the diffusion decision model: Expert advice and recommendations. *Journal of Mathematical Psychology*, *87*, 46–75. http://dx.doi.org/10.1016/j.jmp.2018.09.004.

Bose, T., Bottom, F., Reina, A., & Marshall, J. A. R. (2020). Frequency-sensitivity and magnitude-sensitivity in decision-making: Predictions of a theoretical model-based study. *Computational Brain & Behavior*, *3*(1), 66–85. http://dx.doi.org/10.1007/s42113-019-00031-4.

Botvinick, M. M., Braver, T. S., Barch, D. M., Carter, C. S., & Cohen, J. D. (2001). Conflict monitoring and cognitive control. *Psychological Review*, *108*(3), 624–652. http://dx.doi.org/10.1037/0033-295X.108.3.624.

Brunton, B. W., Botvinick, M. M., & Brody, C. D. (2013). Rats and humans can optimally accumulate evidence for decision-making. *Science*, *340*(6128), 95–98. http://dx.doi.org/10.1126/science.1233912.

Cavanagh, S. E., Malalasekera, W. M. N., Miranda, B., Hunt, L. T., & Kennerley, S. W. (2019). Visual fixation patterns during economic choice reflect covert valuation processes that emerge with learning. *Proceedings of the National Academy of Sciences*, *116*(45), 22795–22801. http://dx.doi.org/10.1073/pnas.1906662116.

Cavanagh, J. F., Wiecki, T. V., Cohen, M. X., Figueroa, C. M., Samanta, J., Sherman, S. J., et al. (2011). Subthalamic nucleus stimulation reverses mediofrontal influence over decision threshold. *Nature Neuroscience*, *14*(11), 1462–1467. http://dx.doi.org/10.1038/nn.2925.

Cavanagh, J. F., Wiecki, T. V., Kochar, A., & Frank, M. J. (2014). Eye tracking and pupillometry are indicators of dissociable latent decision processes. *Journal of Experimental Psychology: General*, *143*(4), 1476–1488. http://dx.doi.org/10.1037/a0035813.

Chabris, C. F., Morris, C. L., Taubinsky, D., Laibson, D., & Schuldt, J. P. (2009). The allocation of time in decision-making. *Journal of the European Economic Association*, *7*(2–3), 628–637. http://dx.doi.org/10.1162/JEEA.2009.7.2-3.628.

Chen, F., & Krajbich, I. (2018). Biased sequential sampling underlies the effects of time pressure and delay in social decision making. *Nature Communications*, *9*(1), 3557. http://dx.doi.org/10.1038/s41467-018-05994-9.

Clithero, J. A. (2018). Response times in economics: Looking through the lens of sequential sampling models. *Journal of Economic Psychology*, *69*, 61–86. http://dx.doi.org/10.1016/j.joep.2018.09.008.

De Martino, B., Fleming, S. M., Garrett, N., & Dolan, R. J. (2013). Confidence in value-based choice. *Nature Neuroscience*, *16*(1), 105–110. http://dx.doi.org/10.1038/nn.3279.

Diederich, A. (2003). MDFT account of decision making under time pressure. *Psychonomic Bulletin & Review*, *10*(1), 157–166. http://dx.doi.org/10.3758/BF03196480.

Dutilh, G., & Rieskamp, J. (2016). Comparing perceptual and preferential decision making. *Psychonomic Bulletin & Review*, *23*(3), 723–737. http://dx.doi.org/10.3758/s13423-015-0941-1.

Fiedler, S., & Glöckner, A. (2015). Attention and moral behavior. *Current Opinion in Psychology*, *6*, 139–144. http://dx.doi.org/10.1016/j.copsyc.2015.08.008.

Fisher, G. (2017). An attentional drift diffusion model over binary-attribute choice. *Cognition*, *168*, 34–45. http://dx.doi.org/10.1016/j.cognition.2017.06.007.

Folke, T., Jacobsen, C., Fleming, S. M., & De Martino, B. (2016). Explicit representation of confidence informs future value-based decisions. *Nature Human Behaviour*, *1*(1), 1–8. http://dx.doi.org/10.1038/s41562-016-0002.

Fontanesi, L., Gluth, S., Spektor, M. S., & Rieskamp, J. (2019). A reinforcement learning diffusion decision model for value-based decisions. *Psychonomic Bulletin & Review*, *26*(4), 1099–1121. http://dx.doi.org/10.3758/s13423-018-1554-2.

Frömer, R., & Shenhav, A. (2019). Spatiotemporally distinct neural mechanisms underlie our reactions to and comparison between value-based options. *BioRxiv*, Article 609198. http://dx.doi.org/10.1101/609198.

Ghaffari, M., & Fiedler, S. (2018). The power of attention: Using eye gaze to predict other-regarding and moral choices. *Psychological Science*, *29*(11), 1878–1889. http://dx.doi.org/10.1177/0956797618799301.

Glickman, M., Sharoni, O., Levy, D. J., Niebur, E., Stuphorn, V., & Usher, M. (2019). The formation of preference in risky choice. *PLoS Computational Biology*, *15*(8), Article e1007201. http://dx.doi.org/10.1371/journal.pcbi.1007201.

Gluth, S., Kern, N., Kortmann, M., & Vitali, C. L. (2020). Value-based attention but not divisive normalization influences decisions with multiple alternatives. *Nature Human Behaviour*, *4*(6), 634–645. http://dx.doi.org/10.1038/s41562-020-0822-0.

Gluth, S., Spektor, M. S., & Rieskamp, J. (2018). Value-based attentional capture affects multi-alternative decision making. *ELife*, *7*, Article e39659. http://dx.doi.org/10.7554/eLife.39659.

Green, N., Biele, G. P., & Heekeren, H. R. (2012). Changes in neural connectivity underlie decision threshold modulation for reward maximization. *Journal of Neuroscience*, *32*(43), 14942–14950. http://dx.doi.org/10.1523/JNEUROSCI.0573-12.2012.

Gwinn, R., Leber, A. B., & Krajbich, I. (2019). The spillover effects of attentional learning on value-based choice. *Cognition*, *182*, 294–306. http://dx.doi.org/10.1016/j.cognition.2018.10.012.

Hare, T. A., Schultz, W., Camerer, C. F., O'Doherty, J. P., & Rangel, A. (2011). Transformation of stimulus value signals into motor commands during simple choice. *Proceedings of the National Academy of Sciences*, *108*(44), 18120–18125. http://dx.doi.org/10.1073/pnas.1109322108.

Helfer, P., & Shultz, T. R. (2014). The effects of nutrition labeling on consumer food choice: A psychological experiment and computational model. *Annals of the New York Academy of Sciences*, *1331*(1), 174–185. http://dx.doi.org/10.1111/nyas.12461.

Hunt, L. T., Kolling, N., Soltani, A., Woolrich, M. W., Rushworth, M. F. S., & Behrens, T. E. J. (2012). Mechanisms underlying cortical activity during value-guided choice. *Nature Neuroscience*, *15*(3), 470–476. http://dx.doi.org/10.1038/nn.3017.

Hunt, L. T., Malalasekera, W. M. N., de Berker, A. O., Miranda, B., Farmer, S. F., Behrens, T. E. J., et al. (2018). Triple dissociation of attention and decision computations across prefrontal cortex. *Nature Neuroscience*, *21*(10), 1471–1481. http://dx.doi.org/10.1038/s41593-018-0239-5.

Jamieson, D. G., & Petrusic, W. M. (1977). Preference and the time to choose. *Organizational Behavior & Human Performance*, *19*(1), 56–67. http://dx.doi.org/10.1016/0030-5073(77)90054-X.

Johnson, J. G., & Busemeyer, J. R. (2016). A computational model of the attention process in risky choice. *Decision*, *3*(4), 254. http://dx.doi.org/10.1037/dec0000050.

Konovalov, A., & Krajbich, I. (2019). Revealed strength of preference: Inference from response times. *Judgment and Decision Making*, *14*(4), 381–394.

Konovalov, A., & Krajbich, I. (2020). Mouse tracking reveals structure knowledge in the absence of model-based choice. *Nature Communications*, *11*(1), 1893. http://dx.doi.org/10.1038/s41467-020-15696-w.

Krajbich, I. (2019). Accounting for attention in sequential sampling models of decision making. *Current Opinion in Psychology*, *29*, 6–11. http://dx.doi.org/10.1016/j.copsyc.2018.10.008.

Krajbich, I., Armel, C., & Rangel, A. (2010). Visual fixations and the computation and comparison of value in simple choice. *Nature Neuroscience*, *13*(10), 1292–1298. http://dx.doi.org/10.1038/nn.2635.

Kvam, P. D., & Pleskac, T. J. (2016). Strength and weight: The determinants of choice and confidence. *Cognition*, *152*, 170–180. http://dx.doi.org/10.1016/j.cognition.2016.04.008.

Lerche, V., Voss, A., & Nagler, M. (2017). How many trials are required for parameter estimation in diffusion modeling? A comparison of different optimization criteria. *Behavior Research Methods*, *49*(2), 513–537. http://dx.doi.org/10.3758/s13428-016-0740-2.

Lim, S.-L., O'Doherty, J. P., & Rangel, A. (2011). The decision value computations in the vmpfc and striatum use a relative value code that is guided by visual attention. *Journal of Neuroscience*, *31*(37), 13214–13223. http://dx.doi.org/10.1523/JNEUROSCI.1246-11.2011.

McGinty, V. B. (2019). Overt attention toward appetitive cues enhances their subjective value, independent of orbitofrontal cortex activity. *ENeuro*, *6*(6), http://dx.doi.org/10.1523/ENEURO.0230-19.2019.

McGinty, V. B., Rangel, A., & Newsome, W. T. (2016). Orbitofrontal cortex value signals depend on fixation location during free viewing. *Neuron*, *90*(6), 1299–1311. http://dx.doi.org/10.1016/j.neuron.2016.04.045.

Merkel, A. L., & Lohse, J. (2019). Is fairness intuitive? An experiment accounting for subjective utility differences under time pressure. *Experimental Economics*, *22*(1), 24–50. http://dx.doi.org/10.1007/s10683-018-9566-3.

Milosavljevic, M., Malmaud, J., Huth, A., Koch, C., & Rangel, A. (2010). The drift diffusion model can account for the accuracy and reaction time of value-based choices under high and low time pressure. *Judgment and Decision Making*, *5*(6), 437–449. http://dx.doi.org/10.2139/ssrn.1901533.

Newell, B. R., & Le Pelley, M. E. (2018). Perceptual but not complex moral judgments can be biased by exploiting the dynamics of eye-gaze. *Journal of Experimental Psychology: General*, *147*(3), 409–417. http://dx.doi.org/10.1037/xge0000386.

Pärnamets, P., Johansson, P., Hall, L., Balkenius, C., Spivey, M. J., & Richardson, D. C. (2015). Biasing moral decisions by exploiting the dynamics of eye gaze. *Proceedings of the National Academy of Sciences*, *112*(13), 4170–4175. http://dx.doi.org/10.1073/pnas.1415250112.

Philiastides, M. G., & Ratcliff, R. (2013). Influence of branding on preference-based decision making. *Psychological Science*, *24*(7), 1208–1215. http://dx.doi.org/10.1177/0956797612470701.

Pirrone, A., Azab, H., Hayden, B. Y., Stafford, T., & Marshall, J. A. R. (2018). Evidence for the speed–value trade-off: Human and monkey decision making is magnitude sensitive. *Decision*, *5*(2), 129–142. http://dx.doi.org/10.1037/dec0000075.

Pirrone, A., Wen, W., & Li, S. (2018). Single-trial dynamics explain magnitude sensitive decision making. *BMC Neuroscience*, *19*(1), 54. http://dx.doi.org/10.1186/s12868-018-0457-5.

Pisauro, M. A., Fouragnan, E., Retzler, C., & Philiastides, M. G. (2017). Neural correlates of evidence accumulation during value-based decisions revealed via simultaneous EEG-fMRI. *Nature Communications*, *8*(1), 15808. http://dx.doi.org/10.1038/ncomms15808.

Polanía, R., Krajbich, I., Grueschow, M., & Ruff, C. C. (2014). Neural oscillations and synchronization differentially support evidence accumulation in perceptual and value-based decision making. *Neuron*, *82*(3), 709–720. http://dx.doi.org/10.1016/j.neuron.2014.03.014.

Ratcliff, R. (1978). A theory of memory retrieval. *Psychological Review*, *85*(2), 59–108. http://dx.doi.org/10.1037/0033-295X.85.2.59.

Ratcliff, R., & Childers, R. (2015). Individual differences and fitting methods for the two-choice diffusion model of decision making. *Decision*, *2*(4), 237–279. http://dx.doi.org/10.1037/dec0000030.

Ratcliff, R., & Frank, M. J. (2012). Reinforcement-based decision making in corticostriatal circuits: Mutual constraints by neurocomputational and diffusion models. *Neural Computation*, *24*(5), 1186–1229. http://dx.doi.org/10.1162/NECO_a_00270.

Ratcliff, R., & McKoon, G. (2008). The diffusion decision model: Theory and data for two-choice decision tasks. *Neural Computation*, *20*(4), 873–922. http://dx.doi.org/10.1162/neco.2008.12-06-420.

Ratcliff, R., & McKoon, G. (2018). Modeling numerosity representation with an integrated diffusion model. *Psychological Review*, *125*(2), 183–217. http://dx.doi.org/10.1037/rev0000085.

Ratcliff, R., & Smith, P. L. (2004). A comparison of sequential sampling models for two-choice reaction time. *Psychological Review*, *111*(2), 333. http://dx.doi.org/10.1037/0033-295X.111.2.333.

Ratcliff, R., & Tuerlinckx, F. (2002). Estimating parameters of the diffusion model: Approaches to dealing with contaminant reaction times and parameter variability. *Psychonomic Bulletin & Review*, *9*(3), 438–481. http://dx.doi.org/10.3758/BF03196302.

Ratcliff, R., Voskuilen, C., & McKoon, G. (2018). Internal and external sources of variability in perceptual decision-making. *Psychological Review*, *125*(1), 33–46. http://dx.doi.org/10.1037/rev0000080.

Ratcliff, R., Voskuilen, C., & Teodorescu, A. (2018). Modeling 2-alternative forced-choice tasks: Accounting for both magnitude and difference effects. *Cognitive Psychology*, *103*, 1–22. http://dx.doi.org/10.1016/j.cogpsych.2018.02.002.

van Ravenzwaaij, D., Donkin, C., & Vandekerckhove, J. (2017). The EZ diffusion model provides a powerful test of simple empirical effects. *Psychonomic Bulletin & Review*, *24*(2), 547–556. http://dx.doi.org/10.3758/s13423-016-1081-y.

Rodriguez, C. A., Turner, B. M., & McClure, S. M. (2014). Intertemporal choice as discounted value accumulation. *PLoS One*, *9*(2), Article e90138. http://dx.doi.org/10.1371/journal.pone.0090138.

Roe, R. M., Busemeyer, J. R., & Townsend, J. T. (2001). Multialternative decision field theory: A dynamic connectionst model of decision making. *Psychological Review*, *108*(2), 370–392. http://dx.doi.org/10.1037/0033-295X.108.2.370.

Sepulveda, P., Usher, M., Davies, N., Benson, A. A., Ortoleva, P., & De Martino, B. (2020). Visual attention modulates the integration of goal-relevant evidence and not value. *ELife*, *9*, Article e60705. http://dx.doi.org/10.7554/eLife.60705.

Shenhav, A., Botvinick, M. M., & Cohen, J. D. (2013). The expected value of control: An integrative theory of anterior cingulate cortex function. *Neuron*, *79*(2), 217–240. http://dx.doi.org/10.1016/j.neuron.2013.07.007.

Shenhav, A., Straccia, M. A., Cohen, J. D., & Botvinick, M. M. (2014). Anterior cingulate engagement in a foraging context reflects choice difficulty, not foraging value. *Nature Neuroscience*, *17*(9), 1249–1254. http://dx.doi.org/10.1038/nn.3771.

Shimojo, S., Simion, C., Shimojo, E., & Scheier, C. (2003). Gaze bias both reflects and influences preference. *Nature Neuroscience*, *6*(12), 1317–1322. http://dx.doi.org/10.1038/nn1150.

Smith, S. M., & Krajbich, I. (2018). Attention and choice across domains. *Journal of Experimental Psychology: General*, *147*(12), 1810–1826. http://dx.doi.org/10.1037/xge0000482.

Smith, S. M., Krajbich, I., & Webb, R. (2019). Estimating the dynamic role of attention via random utility. *Journal of the Economic Science Association*, *5*(1), 97–111. http://dx.doi.org/10.1007/s40881-019-00062-4.

Smith, Philip L., & Ratcliff, R. (2009). An integrated theory of attention and decision making in visual signal detection. *Psychological Review*, *116*(2), 283. http://dx.doi.org/10.1037/a0015156.

Spiegelhalter, D. J., Best, N. G., Carlin, B. P., & Linde, A. V. D. (2002). Bayesian measures of model complexity and fit. *Journal of the Royal Statistical Society. Series B. Statistical Methodology*, *64*(4), 583–639. http://dx.doi.org/10.1111/1467-9868.00353.

Stewart, N., Chater, N., & Brown, G. D. A. (2006). Decision by sampling. *Cognitive Psychology*, *53*(1), 1–26. http://dx.doi.org/10.1016/j.cogpsych.2005.10.003.

Stewart, N., Gächter, S., Noguchi, T., & Mullett, T. L. (2016). Eye movements in strategic choice. *Journal of Behavioral Decision Making*, *29*(2–3), 137–156. http://dx.doi.org/10.1002/bdm.1901.

Stewart, N., Hermens, F., & Matthews, W. J. (2016). Eye movements in risky choice. *Journal of Behavioral Decision Making*, *29*(2–3), 116–136. http://dx.doi.org/10.1002/bdm.1854.

Sullivan, N., Hutcherson, C., Harris, A., & Rangel, A. (2015). Dietary self-control is related to the speed with which attributes of healthfulness and tastiness are processed. *Psychological Science*, *26*(2), 122–134. http://dx.doi.org/10.1177/0956797614559543.

Tavares, G., Perona, P., & Rangel, A. (2017). The attentional drift diffusion model of simple perceptual decision-making. *Frontiers in Neuroscience*, 11. http://dx.doi.org/10.3389/fnins.2017.00468.

Teodorescu, A. R., Moran, R., & Usher, M. (2016). Absolutely relative or relatively absolute: Violations of value invariance in human decision making. *Psychonomic Bulletin & Review*, *23*(1), 22–38. http://dx.doi.org/10.3758/s13423-015-0858-8.

Thomas, A. W., Molter, F., Krajbich, I., Heekeren, H. R., & Mohr, P. N. C. (2019). Gaze bias differences capture individual choice behaviour. *Nature Human Behaviour*, *3*(6), 625–635. http://dx.doi.org/10.1038/s41562-019-0584-8.

Towal, R. B., Mormann, M., & Koch, C. (2013). Simultaneous modeling of visual saliency and value computation improves predictions of economic choice. *Proceedings of the National Academy of Sciences of the United States of America*, *110*(40), E3858–E3867. http://dx.doi.org/10.1073/pnas.1304429110.

Tversky, A., & Kahneman, D. (1979). Prospect theory: An analysis of decision under risk. *Econometrica*, *47*(2), 263–291.

Vaidya, A. R., & Fellows, L. K. (2015). Testing necessary regional frontal contributions to value assessment and fixation-based updating. *Nature Communications*, *6*(1), 10120. http://dx.doi.org/10.1038/ncomms10120.

Vassena, E., Deraeve, J., & Alexander, W. H. (2020). Surprise, value and control in anterior cingulate cortex during speeded decision-making. *Nature Human Behaviour*, *4*(4), 412–422. http://dx.doi.org/10.1038/s41562-019-0801-5.

Von Neumann, J., & Morgenstern, O. (1944). *Theory of games and economic behavior*. Princeton University Press, WorldCat.org.

Wagenmakers, E.-J., Lodewyckx, T., Kuriyal, H., & Grasman, R. (2010). BayesIan hypothesis testing for psychologists: A tutorial on the savage–dickey method. *Cognitive Psychology*, *60*(3), 158–189. http://dx.doi.org/10.1016/j.cogpsych.2009.12.001.

Webb, R. (2018). The (neural) dynamics of stochastic choice. *Management Science*, *65*(1), 230–255. http://dx.doi.org/10.1287/mnsc.2017.2931.

Westbrook, A., Bosch, R. van den, Määttä, J. I., Hofmans, L., Papadopetraki, D., Cools, R., et al. (2020). Dopamine promotes cognitive effort by biasing the benefits versus costs of cognitive work. *Science*, *367*(6484), 1362–1366. http://dx.doi.org/10.1126/science.aaz5891.

Wiecki, T. V., Sofer, I., & Frank, M. J. (2013). Hddm: Hierarchical Bayesian estimation of the drift-diffusion model in python. *Frontiers in Neuroinformatics*, 7. http://dx.doi.org/10.3389/fninf.2013.00014.